Mechanical characterization and crack propagation in Additively Manufactured Polymers using Digital Image Correlation: a review

Hachimi Taoufik
Ecole Normale Supérieure (ENS), Moulay Ismaïl University, BP. 3104, Toulal, Meknes, Morocco
Laboratory of Nuclear, Atomic, Molecular, Mechanical and Energetic Physics, University Chouaib Doukkali, El Jadida, Morocco
Hachtaoufik@gmail.com, https://orcid.org/0000-0002-3567-8511

Zekriti Najat, Ait Hmazi Fouad, Bagar Hamza, El Assad Hatim, Naboulsi Nassima
Laboratory of Nuclear, Atomic, Molecular, Mechanical, and Energetic Physics, University Chouaib Doukkali, El Jadida, Morocco
Najat.ze@hotmail.fr
Aithmazi.f@ucd.ac.ma, https://orcid.org/0009-0009-6919-5540
Bagar.h@ucd.ac.ma, Hatimelassad2@gmail.com, Naboulsi.n@ucd.ac.ma

ABSTRACT. While Additive Manufacturing (AM) of polymers has matured from rapid prototyping to functional production, the layer-wise fabrication process introduces significant mechanical anisotropy and microstructural heterogeneity, which complicates conventional mechanical characterization. This review examines the applicability of Digital Image Correlation (DIC) as a full-field, non-contact metrological tool for mapping strain with sub-pixel precision across three domains: (1) the fundamental metrological principles of DIC applied to anisotropic AM structures, (2) a critical synthesis of DIC applications in tensile, fracture, fatigue, and impact testing, and (3) emerging advances in data acquisition, including in-situ monitoring and AI-driven frameworks. DIC uniquely enables the direct visualization of localized strain concentrations at filament interfaces and non-ideal crack propagation paths that conventional point-wise sensors obscure. Technological maturation is increasingly driven by Deep DIC frameworks and neural operators (DisplacementNet, StrainNet), which now integrate with automated defect tracking systems. Furthermore, multimodal approaches combining DIC with Acoustic Emission (AE) and Micro-Computed Tomography (μ-CT), alongside volumetric Digital Volume Correlation (DVC), extend damage characterization from surface observations to internal defect evolution. To support industrial certification in safety-critical sectors, the community must adopt standardized metrological baselines, including the Metrological Efficiency Indicator (MEI) and the iDICs Good Practices Guide. These

Citation: Hachimi, T., Zekriti, N., Ait Hmazi, F., Bagar, H, El Assad, H., Naboulsi, N., Mechanical characterization and crack propagation in Additively Manufactured Polymers using Digital Image Correlation: a review, Fracture and Structural Integrity, 77 (2026) 173-206.

Received: 11.04.2026
Accepted: 24.04.2026
Published: 25.04.2026
Issue: 07.2026

protocols will bridge the gap between as-designed simulations and as-built experimental validation, positioning DIC as a foundational technology for Industry 4.0 and NDE 4.0 paradigms.

KEYWORDS. Digital Image Correlation, Additive Manufacturing, 3D-Printed Polymers, Fracture Mechanics, Machine Learning, Structural Health Monitoring, Metrological Standardization.

INTRODUCTION

The advancement of additive manufacturing (AM) or three-dimensional (3D) printing from rapid prototyping (1980s) to AM as a disruptive manufacturing method (fabricating components previously infeasible via traditional subtractive manufacturing processes) has greatly changed the way we can produce highly complex, optimized components [5,96]. The ability to provide unprecedented levels of design freedom, mass customization, and large decreases in raw-material waste has led to AM being considered one of the primary drivers of the Industry 4.0 revolution [73,110]. The largest segment (by volume) of materials used in AM is polymers due to cost-effectiveness, ease of processing, and wide applicability in aerospace, biomedical, automotive, and electronics industry applications [5,48]. The current AM technologies that dominate the ecosystem of AM include Material Extrusion (FFF), Vat Photopolymerization (SLA/DLP), and Powder Bed Fusion (SLS) [73]. Of these, FFF is the most accessible and widely used in industry with thermoplastic filament materials such as PLA, ABS, and high-performance PEEK materials [40,73,74] While the SLA/DLP process has better surface finish and dimensional tolerances than FFF is used in approximately 50% of all industrial prototyping [77]
Despite advances in metallic and ceramic additive manufacturing, polymer-based AM presents unique measurement challenges. These materials exhibit strong anisotropy, weak inter-layer bonding, micro-voids, and residual stresses, leading to localized and non-uniform failure mechanisms that traditional techniques cannot capture. As a result, Digital Image Correlation (DIC) has become essential for analyzing strain fields at the mesostructural scale. Focusing on AM polymers enables targeted investigation of process–structure–property relationships, speckle optimization, and validation of anisotropic models specific to printed thermoplastics and photopolymers. While these technologies have advanced, the layer-by-layer deposition method that is fundamental to AM has created critical microstructural complexity that contradicts what engineers' assumptions regarding how conventional engineering principles apply to these types of materials [24,44]. 3D Printed polymers are mechanically anisotropic (dramatically different mechanical strengths via different orientations), have interlayer voids, and process-induced residual stresses that control how the 3D Printed polymer will fail (initiation of failure and propagation) [6,24,44]. The arising complexities of polymer microstructure can be attributed to the mechanisms of 3D printing; specifically, how component temperature-driven diffusion is occurring through the interface of individual 3D printed beads (as beads cool) due to the properties of polymers, the linear, directional raster pattern used to create the bead; along with the cooling profiles for each bead created require 3D printed polymer to respond fundamentally differently depending on how the part was oriented in terms of how the toolpath was created [24,45]. As a result of these complexities, many of the standard point-wise methods of characterizing and measuring these materials, including mechanical extensometers and electrical resistance strain gauges, have increasingly proven insufficient [45]. These averaging techniques suppose that deformation exhibits some form of uniform stress behaviour throughout a prescribed gauge length, effectively averaging out small-scale strain concentrations [110]. In AM-designed polymers, for instance, initiation of failure often occurs at microscopic voids between beads or within layers, or the failure process may preferentially travel along weak inter-layer fracture surfaces. Single-point measurements hide key strain events progressing through a component and are biased due to contact with low-stiffness specimens [2,44,110].
To solve this metrological challenge, Digital Image Correlation DIC emerges as the most significant of non-contact, full-field optical measurement solutions in experimental mechanics [91,116]. DIC tracks the displacement of a random speckle across consecutive digital images dependent on mechanical loading to create a high-resolution 2D and 3D displacement and strain map with subpixel-level accuracy [81,116]. Since its first establishment in the early 1980s, the technique has matured via further development in computational algorithms and image processing, imaging hardware, and correlation criteria [99]. Unlike conventional sensors, DIC reveals the overall kinematic response structure as dictated by the internal architecture of the part, for example, allowing hot spots of strain concentration, evolution of crack paths, and quantitative compliance to anisotropic constitutive modelling [6,22,84]. The techniques' natural applicability to quasi-static and dynamic loading

approaches and their benign integration with experimental workflows have collectively established it as indispensable for the characterisation of process-structure-property relationships in additively manufactured polymers Figure 1 [22,120].

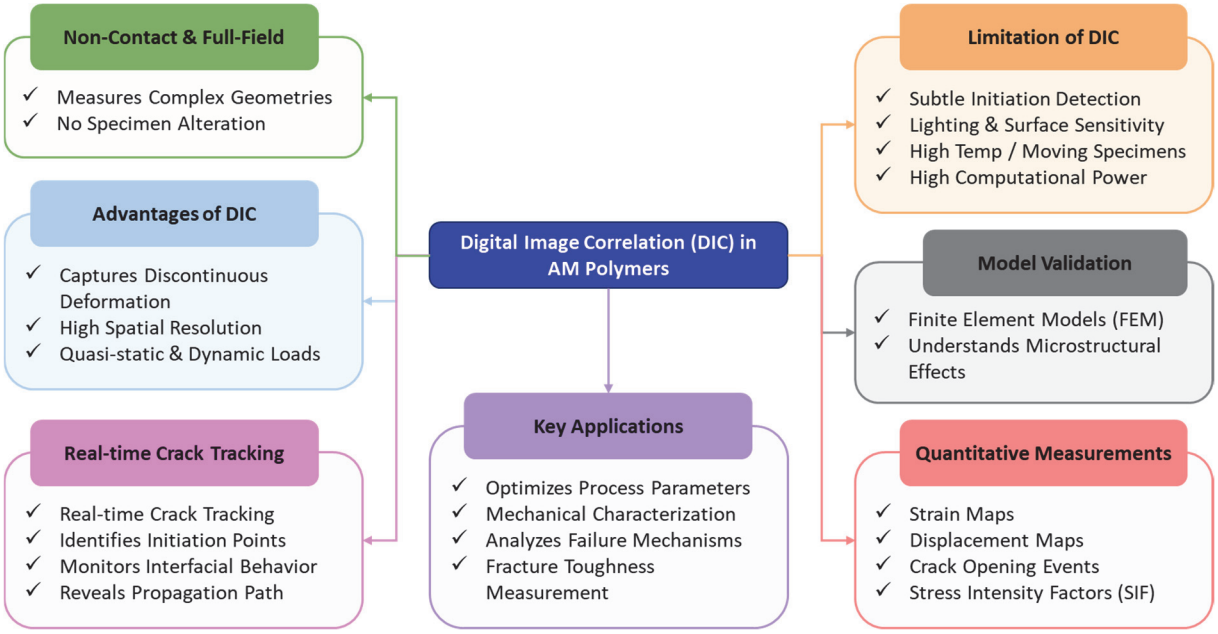

Figure 1: Multifaceted applications, advantages, and limitations of Digital Image Correlation (DIC) in the study of additively manufactured polymers.

Perhaps one of the most enriching applications lies in fracture mechanics and crack propagation analysis [50,115]. As the field of additive manufacturing (AM) migrates towards producing multi-material structures and architected lattice metamaterials, the need for spatially resolved data is growing [79,88]. In polymers, for example, where the strain localisation occurs at the "neck" between deposited beads, using too large a subset can smooth over critical data and result in derived peak strains being below those that are typically required for accurate fracture modelling [2,91]. High-impact work in this area typically involves the adoption of optimised algorithms such as Zero-mean Normalised Sum of Squared Differences (ZNSSD) correlation, where the correlation criterion remains more consistent and robust under rapidly fluctuating lighting conditions typical of in-situ AM work being carried out at high pace [22,82,83]. Multi-material AM also introduces, in certain cases, the risks from the joining of chemically incompatible materials in certain locations that appear optimal for joining yet separate or "delaminate" during strain that is seen to interrupt, subsequent to their joint forming [67,78]. In such cases, DIC is the sole tool for mapping the discontinuity of strain that precedes "delamination" [67,78]. A utility that arises from the combination of DIC with Machine learning (ML) and Deep learning (DL) is curating the movement of defect recognition towards fully automated processes and "agnostic" qualification standard [79,93,112]. These "Deep DIC" frameworks, such as DisplacementNet, can "directly" predict the deformation field from the image data without further noise amplification that typically arises through numerical differentiation [79,112,118]. While surface-based approaches yield a plethora of information, the line-of-sight properties of these approaches mean that DIC sister techniques, Digital Volume Correlation (DVC), and exploiting Micro-CT data in particular, are used to map 3D strain invariants throughout the volume of much of the part [41,103]. This holistic approach allows for the first-time visualization of how internal porosity and raster geometry interact with macroscopic loads to govern the failure of additively manufactured composites[41,103].

Despite the growing frontier of this literature in general, there remains no specific review detailing the synergy of DIC & 3D-printed polymers in particular[22]. Many papers focus on either metallic AM or DIC theory(ies) generally, or polymer mechanics without adapting the core to address what significantly makes AM polymers different, such as topography/viscoelastic behavior/multilayers affecting the mechanics [84,103]. New additions, such as the rapid embedding of AI, in-situ monitoring frameworks, etc., are not catalogued in the literature [36,62,113]. This review aims to remedy this gap by: (1) reminding readers of the underlying metrological principles and algorithmics behind DIC for a simulacrum of that constrained for the 'normal' case of an isotropic material with perfect surfaces, (2) subsequently reviewing DIC applications in tensile tests, crucible, fractured composites, consistent/uncertain fatigue (defect quantification, basic crack propagation), and fast-impact DIC, and finally (3) articulating pitches for "the future" from micro-scale DIC to multimodal measurements to certifying in international meta-standardisation protocols to move forward towards certifying this to where

it never was: a core application for (safety-relevant) industrial applications. This paper attempts to pull these gains negotiated by other researchers as a clearer whole into a larger logical/conceptual frame with DIC standing/pivotal to tying together what-is-designed and what-is-actually-installed/certified as the respective linkages, to 'map' who should get onto putting in place so that AM polymers/plastics etc can be used safely for safety-deterministic engineering applications.

THEORETICAL FOUNDATIONS AND METROLOGICAL PRINCIPLES OF DIC IN ADDITIVE MANUFACTURING

The advantage of developing a thorough understanding of the mathematical, optical, and metrological principles underlying DIC becomes clear in the context of focusing on the applications of DIC to additively manufactured polymers. Since the printed materials are often heterogeneous and 3D anisotropic (due to factors such as material raster 3D printing paths and interfacing between subsequent layers) [6,24,44]. The performance of the DIC measurement system cannot be expressed in standard instrument specifications but is actually a function of material mesostructure as well [2,91,120].

Historical evolution and core principles

DIC itself has developed through two major phases since Peters and Ranson [86] first considered how speckle could be tracked to yield a 2D-DIC technique, as Sutton et al. [99] implemented random speckle tracking using a Newton-Raphson optimization routine, and now into stereo-DIC and Digital Volume Correlation, which covers engineering scales, allowing full-field (2.5D) mapping of strain over an entire surface [3,41,80,103]. DIC essentially statistically tracks speckles (high-contrast stochastic speckle patterns applied to the specimen surface to optimize correlation parameters in the correlation process, usually the DIC tables make the user choose parameters to be stochastically masked) by matching square subsets between the reference speckled surface and its altered post-deformation state with a mapping function describing the statistical data [59,81]. The technique is non-contact, capable of tracking high-resolution fields of displacement and strain, and requiring no sensors due to allowing just-in-time finite element mesh generation and quantifying localised gradients (Figure 2)[1,84].

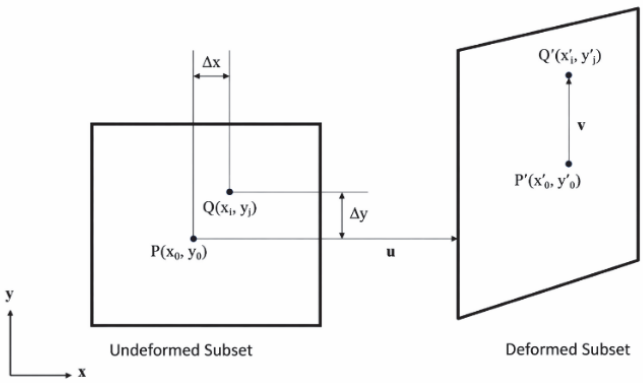

Figure 2: Principle of the subset-based Digital Image Correlation (DIC) method, illustrating reference/deformed image matching and displacement vector calculation.

Mathematical framework and correlation criteria

The general calculation of the displacement occurring at the centre of a subset uses a shape function to model local deformation. For most AM applications, a first-order shape function based on translation, rotation, and normal strains as defined by Equations 1 and 2 above is all that is usually used [2,26].

$$x' = x + u + \frac{\partial u}{\partial x}\Delta x + \frac{\partial u}{\partial y}\Delta y \tag{1}$$

$$y' = y + v + \frac{\partial u}{\partial x}\Delta x + \frac{\partial u}{\partial y}\Delta y \tag{2}$$

where $\Delta x = x - x_0$ and $\Delta y = y - y_0$, u and v represent the displacement components of the subset center, and the partial derivatives correspond to displacement gradients.

In more complicated multi-axial loading regions of interest, such as crack tips in 3D printed lattices, second or higher-order shape functions are needed to accurately represent the distortion and warping of subsets [6,15,88]. The Inverse Compositional Gauss–Newton (IC-GN) is the computational benchmark for solving these well-known nonlinear optimization problems due to its stability and efficiency [81,113]. Strain calculation is more difficult than simple mapping of displacements since spatial differentiation magnifies all noise in measurements; the Green–Lagrangian strain tensor (used in Equation 3) is commonly applied to describe finite deformations that result in a more accurate estimate of the state of strain [11,42,91].

$$
\begin{aligned}
E_{xx} &= \frac{1}{2}\left[2\frac{\partial u}{\partial x} + \left(\frac{\partial u}{\partial x}\right)^2 + \left(\frac{\partial v}{\partial x}\right)^2\right] \\
E_{xy} &= \frac{1}{2}\left[\frac{\partial u}{\partial y} + \frac{\partial v}{\partial x} + \frac{\partial u}{\partial x}\frac{\partial u}{\partial y} + \frac{\partial v}{\partial x}\frac{\partial v}{\partial y}\right] \\
E_{yy} &= \frac{1}{2}\left[2\frac{\partial v}{\partial y} + \left(\frac{\partial u}{\partial y}\right)^2 + \left(\frac{\partial v}{\partial y}\right)^2\right]
\end{aligned}
\tag{3}
$$

To quantify how similar subsets are, non-destructive evaluation practitioners adopted the Zero-mean Normalized Sum of Squared Differences (ZNSSD) as the standard correlation criterion since it is invariant to linear changes in the image intensity and glare changes, e.g., surface lighting (Equation 4) [82,83]. In comparison to the earlier primitive implementation that used the basic Sum of Squared Differences (SSD) [83], ZNSSD is less sensitive to non-uniform illumination arising from in-situ AM monitoring setups [22,62]. The continuous algorithmic improvements ensure improved stability in actual implementations of DIC codes. Tong [104] computed various correlation criteria and subsequently evaluated various criteria, setting initial standards for the DIC community. Schreier et al. [94] show that the use of cubic/ quintic splines for sub-pixel registration reduces systematic bias errors (the difference in the true displacement from the actual displacements due to a poor choice of description functions). Lu and Cary [61] improved displacements' accuracy with full second-order displacement gradients. Schreier and Sutton [95] obtain estimates of the errors from an undermatched shape function in detail. The reliability-guided displacement tracking (RGDT) method improves convergence in those highly distorted fields; this method uses a weight for pixels surrounding a subset to trade accuracy for computational cost. Pan [81] proposes a reliability-guided displacement tracking (RGDT) strategy that optimizes computational efficiency without sacrificing accuracy.

$$
C_{NCC} = \sum_{i=-M}^{M}\sum_{j=-M}^{M}\left[\frac{\sum_{i=-M}^{M}\sum_{j=-M}^{M} f(x_i,y_j)\,g(x'_i,y'_j)}{\sqrt{\sum_{i=-M}^{M}\sum_{j=-M}^{M}\left[f(x_i,y_j)\right]^2 \sum_{i=-M}^{M}\sum_{j=-M}^{M}\left[g(x'_i,y'_j)\right]^2}}\right]
\tag{4}
$$

where $f(x_i,y_j)$ and $g(x'_i,y'_j)$ denote the grayscale intensity values of the reference and deformed images, respectively, and M defines the subset size. The optimal displacement field is obtained by maximizing the NCC coefficient.

Speckle patterning and surface fidelity

A viable stochastic speckle pattern must respect all four of the following critical criteria, viz., being high in contrast, random, isotropic, and must also actively resist the load of adhesion. Reu et al. [91] recommend that speckle sizes of between 3 and 5 pixels should be viewed as very desirable obstacles to avoid 'biasing' the measurements as a result of any aliasing. As a surface, AM polymers offer an array of new contaminants/challenges [84], and difficulty in accurate speckle pattern application and optimization of speckle contrast can also be hindered by factors such as roughness, translucency, and reflectivity. Traditionally, speckles are applied by spray painting, although as noted by Lupone et al. [64], continuous fiber composites and highly textured surfaces are often easier to reach with airbrushing or inkjet printing. Cunha et al. [22] observe

that natural surface textures in PBF processes can be of sufficient contrast to allow meaningful correlation without the need for artificial patterning. Diani et al. [25] directly address this by substituting ink-stamped circular dots for the speckle in a reproducible manner, allowing for better control of speckle morphology, whilst Liu et al. [60] further develop microscale speckle that is resistant to heat for high-temperature AM environments. Wang and Lei [108] utilize deep learning to super-resolve DIC data, allowing for enhanced correlations from lower-res images. With this awareness, specific wood-fiber filaments exist that can form natural speckles during printing processes, as demonstrated by Holzmond and Li [46]ndeed, this trend is towards the more "pattern-agnostic" types of algorithms, which are generally surfacing now. Szalai et al. [100] also show that surface cleaning and priming parameters are just as important as the patterning step itself for effective correlation of complicated structural materials. For conventional macro-scale methods, Dong and Pan [26] show in their proof-of-principle that conventional scratching using sandpaper or dry toner can be used, and by looking at the relative distributions of the greyscale images between the reference and distorted counterparts, the entire displacement field can be reconstructed (Figure 3).

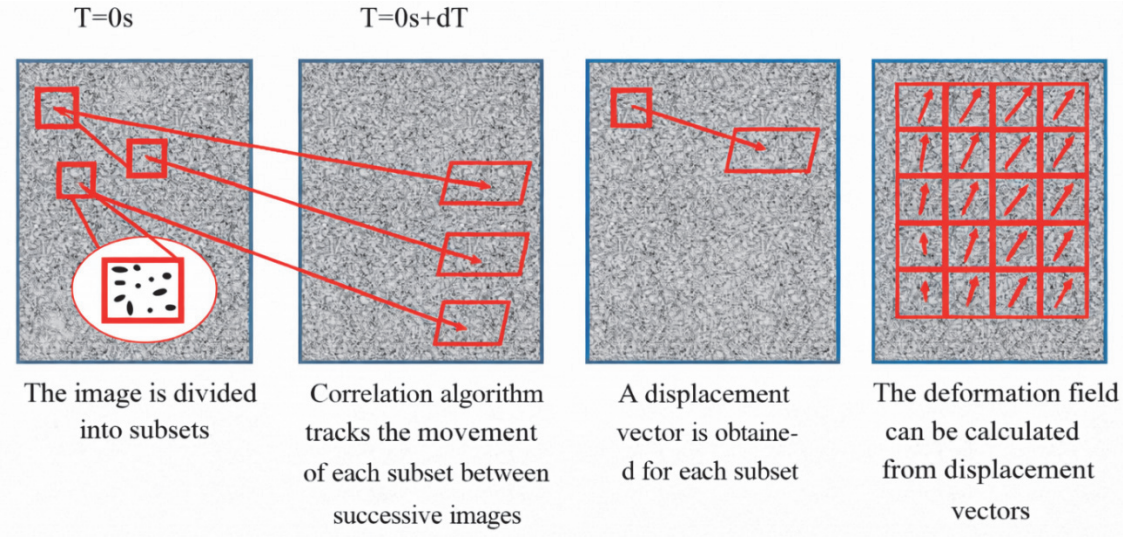

Figure 3: Schematic representation of DIC subset tracking and deformation gradient mapping across a stochastic speckle pattern.

Metrological constraints and spatial resolution

In AM polymer characterisation, a central challenge is the critical trade-off of subset sizes, measurement noise, and resolution [6,91]. The DIC spatial resolution is roughly proportional to subset size, and for first-order shape functions, the displacement resolution is approximately proportional to ~(2M+2) for a subset of (2M+1)×(2M+1) pixels [91]. In polymers like PLA and ABS, Acciaioli et al. [2] and Perez et al. [85] as localised strain occurs at the 'neck' between deposited beads, inappropriately large subsets smooth over critically needed data and severely underestimate the peak strains crucial for proper fracture modelling. As a result of such considerations, we may find in literature that the technical depth is absent in studies that do not report the Metrological Efficiency Indicator (MEI) or, at the very least, perform baseline noise studies to obtain the limiting strain detection capabilities, the importance of which is evident for reliably measuring small elastic strains in stiff, high-performance polymers [91]. A useful summary of such algorithm parameters as they influence the AM characterisation is given in Table 1.

DIC Algorithm Parameter	Impact on AM Characterization	Technical Implication
Subset Size	Signal-to-noise ratio	Larger subsets smooth over filament-level strain concentrations [91]
Step Size	Strain map density	Smaller steps increase the resolution of localized shear bands [2]
Shape Function Order	Accuracy of warping	Higher-order functions are needed for complex lattice strut buckling [2,6]
Correlation Criterion	Lighting invariance	ZNSSD is required for in-situ monitoring with flickering heat sources [2,83]

Table 1: DIC algorithm parameters and their direct impact on AM polymer characterization accuracy.

METHODOLOGY OF APPLYING DIGITAL IMAGE CORRELATION IN POLYMER AM

The experimental workflow of DIC in polymer AM encompasses three intertwined component stages: namely, specimen preparation, the data acquisition through optical processes, and its subsequent computational correlation (Figure 4). Each of these stages requires careful parameter optimisation to the specificised `mesostructural` and surface properties of the 3D printed polymer in order to ensure metrological fidelity.

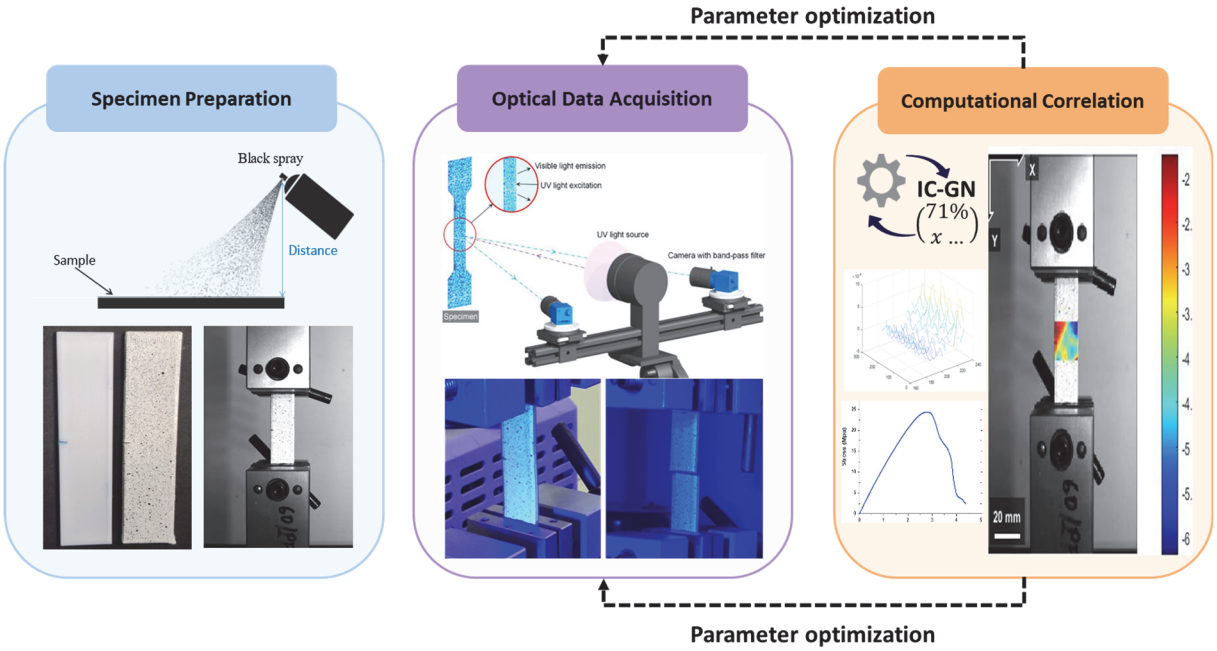

Figure 4: Standardized experimental workflow for DIC application in AM polymer characterization, encompassing specimen preparation, optical acquisition, and computational correlation.

Specimen preparation and surface conditioning

Effective DIC applications necessitate proper application of a high-contrast, randomly scattered speckle pattern that nonetheless remains suitably adherent in all orientations. Lupone et al. [64] and Pellegrini et al. [84] note that application of the speckle pattern is hindered by inherent surface roughness, translucency, or reflectivity that is often found in AM polymers. It is common to spray paint a white base on it, followed by speckling it in a random (black) manner. Lupone et al. [64] believe that airbrushing or inkjet printing would give more ideal results for `continuous fibre composites` and high-texture geometry. To avoid pattern distortion during large deformations, speckle sizes should be tuned to 3-5 pixels to mitigate aliasing-induced measurement errors. Altering the pattern density and subset patch size is critical in capturing localized strain gradients at interlayer interfaces without adding excessive optical noise or concealing micro-defects.

Experimental setup and imaging parameters

Optical acquisition necessitates synchronized high-resolution cameras calibrated relative to the mechanical loading frame. Zouaoui et al. [120] and Tang et al. [101] state that diffused lighting must be implemented to avoid glare and shadow artefacts on polymeric surfaces. tensile/bending tests, low frame rates are sufficient, Zouaoui et al. [120] show that stereo-DIC configurations are essential for taking measurements of warping out-of-plane that naturally occurs in asymmetric AM architectures. High-speed imaging and proper scaling of the images to be captured are necessary to capture dynamic and impact loading, with camera calibration routines requiring extensive validation in order to accurately perform the reconstruction of the 3D strain fields, especially with regard to locating subpixel displacements across complex lattice topologies and non-planar “as-built” surfaces.

Data processing and algorithmic workflows

The acquired image sequences are subjected to subset-based correlation to determine pixel intensity variations from frame to frame. The subset and step parameters must be optimised as they represent a trade-off between spatial fidelity and noise

sensitivity, and should be iteratively tuned for each material architecture. The final post-processed conversion of the displacement vectors into strain fields uses differentiating techniques, making filtering or smoothing approaches necessary to reduce artifacts induced by differentiation. Pahlavani et al. [79] show that applying clustering algorithms to the DIC-derived strain maps permits the classification of microstructural heterogeneity, thus enhancing the potential for homogenisation towards multiscale constitutive modelling. The resulting visualisation pipeline delivers full-field contour maps that span across detected plastic regions indicative of incipient damage zones, affording experimental feedback directly in relation to interpreting failure modes during the classification phases of structural classification methods.

Software ecosystem and computational frameworks

The continuous development of DIC has led to a diverse ecosystem of commercial and open-source software. Blaber et al. [14] used the Ncorr platform, an open-source MATLAB-based tool, to address large deformations in polymers through sequential Region of Interest (ROI) updates. Turner et al. [105] show the capabilities of DICe, another mature open-source platform developed for high-performance kinematic calculations. Venter et al. [106] used SUN-DIC, a Python-based tool, to demonstrate the trend toward extensibility and ease of use in academic research.

Among all these software solutions, the most mature open-source software that is also the easiest to install and use is Ncorr and DICe. Other tools like Pyxel, Pydic, or dolfin_dic are useful but often more research-centered, require further coding work, or simply aren't as intuitive as DIC.

Commercial software solutions

The commercial world of DIC is made up of highly refined, specialized suites of optimized packages and high-end hardware working together to analyze materials, "turn-key" solutions. These packages may not be open-source, but the gold standard in most engineering applications.

- Correlated Solutions, Inc.: One of the most widely used packages, including Vic-2D and Vic-3D software. Well-known in general for how "out of the box" they are, and still modelling using optimized correlation algorithms to present a precise field of displacements or strain.
- GOM: Another industrial company working in the world of measuring 3D coordinates, and their ARAMIS software uses a truly material-independent base approach and is being widely used for analyzing kinematic fields or deformation of materials and bodies.
- Dantec Dynamics: Coming into their 3D DIC system Q-400, but they claim to be active in the flow measurement game as far back as the 50's.
- LaVision: Pressured by their affiliate from the Max Planck Institute, they provide the product, Strain Master. Specifically developed for application as a nonintrusive optical shape and deformation measurement tool, it uses their algorithms with specific imaging hardware.
- HOLO3: Came up with CorreliSTC under the licensing provisions of Airbus Group Innovations for applications, primarily in automotive, aerospace, or safety-critical energy.
- Imetrum markets Video Gauge™, which is frequently utilized in large-scale structural monitoring (e.g., bridges and structures) to identify crack openings and high-stress areas.
- Image Systems offers TEMA software, providing robust tracking for 2D and 3D kinematic fields.
- MatchID provides 2D and 3D DIC software developed by experts specifically for experimental mechanics applications.

Open-source platforms and advanced algorithmic features

The open-source community is anchored by stable tools like Ncorr and DICe, which have enabled democratized access to high-fidelity characterization [91]. Ncorr is a subset-based formulation for 2D CCD cameras written in MATLAB, developed at the Georgia Institute of Technology. It is widely seen as robust for research as well as specific implementation of large-scale deformation tracking [14]. DICe has been developed by Sandia National Laboratories and is a high-performance DIC implementation for 2D and 3D local/global and many volumes. The tool is written in C++ with an easy GUI and allows for advanced post-processing in ParaView. These two codes represent some of the easiest access points for researchers due to their stability and relative ease of installation.

A common difficulty of performing DIC on additively manufactured (AM) polymers like soft elastomers or high-strain thermoplastics is that the specimen undergoes gross shape changes during loading. To enable DIC tracking in these cases, Ncorr uses a strategy of creating composite displacement maps by taking images of intermediate stages sequentially [14]. Specifically, it updates the Region of Interest (ROI) by defining a boundary which it then updates based on displacement

values from the last computed displacement Field (Figure 5). This ensures the deformation between adjacent frames does not exceed a solvable amount, assuming the pattern is adhered well.

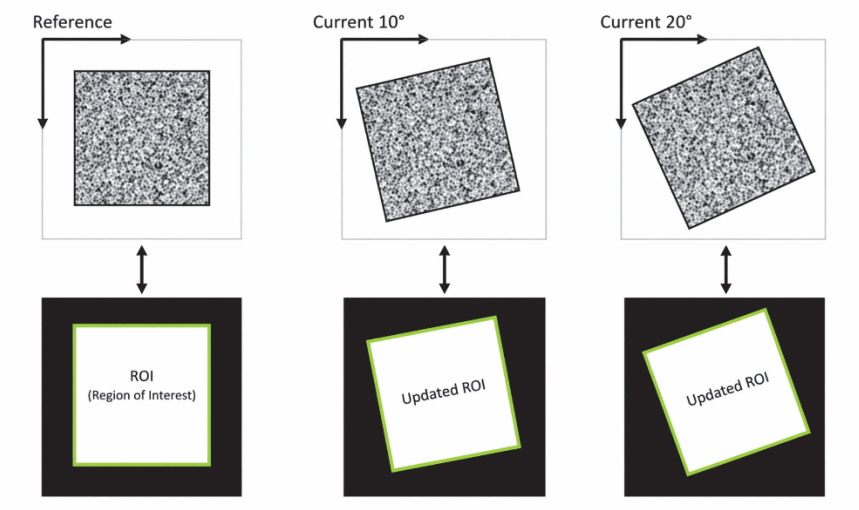

Figure 5: A graphical example of the ROI update scheme.

Research-oriented libraries and emerging frameworks

In addition to mature GUIs, a host of libraries exists for researchers with unique needs, particularly in the context of the Python and C++ ecosystems for scientific computing.

- Ncorr: subset-based 2D digital image correlation software, open-source and free. This software was developed at the Georgia Institute of Technology and is implemented in MATLAB.
- DICe is an open-source DIC software developed by Sandia National Laboratories, capable of calculating displacement and strain fields from a sequence of digital images. It is multi-platform and easy to use; installers are available for Windows and Mac OS, and instructions are provided for building the software on Linux. It has an intuitive graphical user interface for performing 2D and 3D DIC. However, results can easily be post-processed in Paraview, a data analysis and visualization application.
- YaDICs: A C++ platform for Linux that supports both local and global methods combined with pyramidal scales for solid and fluid mechanics.
- Python-Based Tools: This ecosystem includes Pyxel (global 2D library), Pydic (local 2D using OpenCV), Dolfin_dic (global 2D/3D), and Py2DIC.
- SUN-DIC: A Python-based tool known for its extensibility and successful benchmarking against the DIC Challenge 2.0 datasets.
- High-Performance and Specialized Tools: Some newer entries are DICLab2D, which uses the Julia language to implement high-order shape functions for inhomogeneous fields, and icCorrVision-2D, which provides a GUI for selecting the main correlation and calibration parameters.

The intelligent frontier: deep DIC and neural operators

The most notable evolution to recent DIC methodology has seen a marked shift from iterative matching to Deep Learning architectures. Emerging "Deep DIC" frameworks, such as DisplacementNet and StrainNet, provide methods for end-to-end predictive knowledge for deformation fields and avoid the noise amplification present in traditional numerical differentiation, even under large deformations, leading to speckle patterns to tear.

Continuing the thought is DICNO, short for Digital Image Correlation Neural Operator, which maps latent features of a pair of images to a continuous displacement field, suitable for 'one-size-fits-all' across images at different scales. For in-situ monitoring of soft AM parts, the MLF-DICNet applies a multi-level feature fusion strategy, reducing measurement errors by 36.9% relative to traditional iterative methods, and the DICTr leverages Transformer-based feature matching to balance spatial resolution and accuracy of complex patterns in soft AM polymers. A comparison of a few open-source DIC software packages, dimensions, methods used, and other important features pertinent to AM work is listed in Table 2.

Software	2D/3D	Approach	Language / Platform	Key Characteristic	Link / Source
DICe	2D/3D	Local / Global	C++	Intuitive GUI; multi-platform;	GitHub
dolfin_dic	2D/3D	Global	Python	FEM-based DIC; research-oriented	Bitbucket
Ncorr	2D	Local	MATLAB	Robust ROI updates for large deformation	Website
Pydic	2D	Local	Python	Lightweight; easy to use	GitLab
Pyxel	2D	Global	Python	FEM global DIC; strong research usage	GitHub
Py2DIC	2D	Local	Python	Validated vs commercial DIC	GitHub
YaDICs	2D/3D	Local / Global	C++	High-performance; large datasets	Website
iCorrVision	2D	Local	Python	GUI for specific calibration parameters	GitHub
OpenCorr	2D/3D	Local / Global	C++	Modern, high-performance DIC	OpenCorr.org
MultiDIC	3D	Global	MATLAB	Stereo DIC; calibration tools	MIT Media Lab
DuoDIC	3D	(Unspecified, Global)	MATLAB	Stereo DIC; well-documented	JOSS Publication
RealPi2dDIC	2D	Local	Python + Raspberry Pi	Low-cost experimental setup	GitHub / ScienceDirect
Deep DIC	2D	Global (Deep Learning)	Python / DL frameworks	End-to-end DisplacementNet/StrainNet	arXiv
DICNO	2D/3D	Operator	Python	Neural Operator for scale generalization	DICNO
SUN-DIC	2D	Local	Python	Modern Python DIC; GUI + API; Benchmarked against DIC Challenge 2.0	SUN-DIC
DICLab2D	2D	Local	Julia	High-order shape functions (up to 4th order)	DICLab2D

Table 2: Features of Select DIC Open-Source Software.

Standardization and metrological reporting

For the industrial application of DIC, it is necessary to follow established protocols for quantifying uncertainty and preparing reports. Through the DIC Challenge 2.0, Reu et al. [91] created the Metrological Efficiency Indicator (MEI), which quantitatively defines the tradeoff between noise and resolution. To aid in the establishment of uncertainty propagation models for VSGs, Beck [11] and Grédiac et al. [42] summarized the components of an uncertainty propagation model and also provided a means for calculating the sensitivity of the respective hardware to predict system performance of DICs over time. For required operational compliance with ANSI (2026) and ISO 10012:2026 measurement management standards, these requirements have also been established by Jones et al. [51] and outlined in the NCAL/NIST iDICs Good Practices Guide through minimum calibration and reporting requirements. Ahmad et al. [3] validated these standards during the Stereo-DIC Challenge 1.0 by successfully demonstrating that the stated protocols for DIC enable robust evaluation of non-planar AM geometries. These metrological standards serve as the foundation for transitioning DIC from the realm of academic research into that of certified industrial use, which is summarized in Table 3.

Technical Domain	Key Finding	Strategic Insight for AM Certification	Ref
Benchmarking	Established a standardized performance factor for noise-resolution trade-offs.	Essential for the objective comparison of DIC codes across different AM hardware.	[91]
Uncertainty	Formulated predictive noise propagation and uncertainty decay for VSGs.	Provides the mathematical confidence bounds needed for safety-critical certification.	[11,42]
Regulation	Integrated DIC reporting requirements into industrial measurement management.	Moves DIC from an «ad-hoc» research tool to a legally defensible certification method.	[9,51]
Scalability	Open-source platforms achieved performance equivalent to commercial solvers.	Democratizes high-fidelity characterization for SMEs and decentralized production.	[89,106]
Complexity	Validated the ability of stereo-systems to track complex shapes and non-planar motion.	Crucial for qualifying the «as-built» topography of 3D-printed components.	[3]
Deep Learning	Reduced errors by 36.9% and enabled 95% accurate real-time crack tracking.	Facilitates high-throughput, automated quality control in digital twin environments.	[111,113]
Edge Metrology	Improved measurement fidelity at specimen edges and crack fronts.	Allows for accurate quantification of strain at the «neck» of printed road interfaces.	[98]
Data Fusion	Positioned DIC as a passive observer for multimodal damage identification.	Integration with IoT and AI is the prerequisite for next-generation structural health monitoring.	[1]

Table 3: Industrial Metrology and Standardization Trends.

MECHANICAL CHARACTERIZATION OF AM POLYMERS

The mechanical properties of AM components are primarily affected by the layer-by-layer AM building process. Due to the AM process creating a high degree of mechanical anisotropy and mesostructural heterogeneity, the layered nature of the AM components results in mechanical properties being directionally dependent upon the post-processing conditions as they relate to raster pattern, interlayer voids, and infill density. The development of DIC and DVC has been essential in examining the manner in which the three-dimensional distribution of mesostructural parameters affects the mechanical performance of polymer components and how these parameters affect the crack propagation mechanics in these components. By taking advantage of the full field optical methods now available via DIC and developing a method to track crack propagation within AM components, significant insights have been gained into the interactions of mesostructural parameters with respect to crack propagation dynamics and the resultant mechanical properties [110].

Mechanical anisotropy and build orientation effects

Due to the unique deposition method of AM, filament deposition results in inter-bead planes developing a directional orientation (weakness), creating wide variances in strength based on the axis of load application [96]. In this study, Shahan et al. [97] illustrate that the loading orientation of the raster pattern has a significantly greater impact on strength than that of infill percentage (over 40% reduction in flexibility for a raster angle of 90 degrees in both PLA and ABS). Alternatively, Seifollahi and Kabir [96] use DIC to show that on-edge (YZ) build orientations enhance tensile strength by 19% vs. flat-printed specimens due to attenuated micro-void density and improved layer fusion. Albaşkara and Yıldız [4] further note that while horizontally printed grid networks yield optimal strength vs. ductility for PLA, triangular patterns enhance strength for PETG. Further quantifying the mechanical sensitivity to loading axis are Machado and Cardoso [66], who used Classical Lamination Theory to show that deviations in elastic moduli of ABS were significantly greater in line deposition patterns than in grid. Combining modelling with DIC, Rahman et al. [90] found that upright build orientations reliably had the lowest axial strength in micro-carbon fibre reinforced Nylon 6 and ABS due to layer interfaces perpendicular to the

load. Ali et al. [6] combined DIC with desirability function analysis, quantifying that infill density accounts for 48.61% of overall strength, visualizing bimodal strain distributions in upright specimens that reveal stress concentrations due to voids between layers, and reporting a 2.08% performance gain with optimised parameters. Netto et al. [76] noted that Microstructural features of a part, such as voids and the raster-interface Heterogeneity, and the Fibre Misalignment of FFF, ultimately required unique identification of configuration-specific damage parameters. Importantly, Fisher et al. [34] recognized that the orientation of a part during the characterization of the material will significantly influence the Predictive Accuracy of Numerical Impact Models. Generalising this to short-fibre systems, Fisher et al. [33] showed that tensile performance in Onyx composites is controlled by infill orientation, and DIC analysis showed that off-axis raster patterns favour infill rotation during tension. The relative mechanical performances with respect to variations of the parameters are collated in Figure 6.

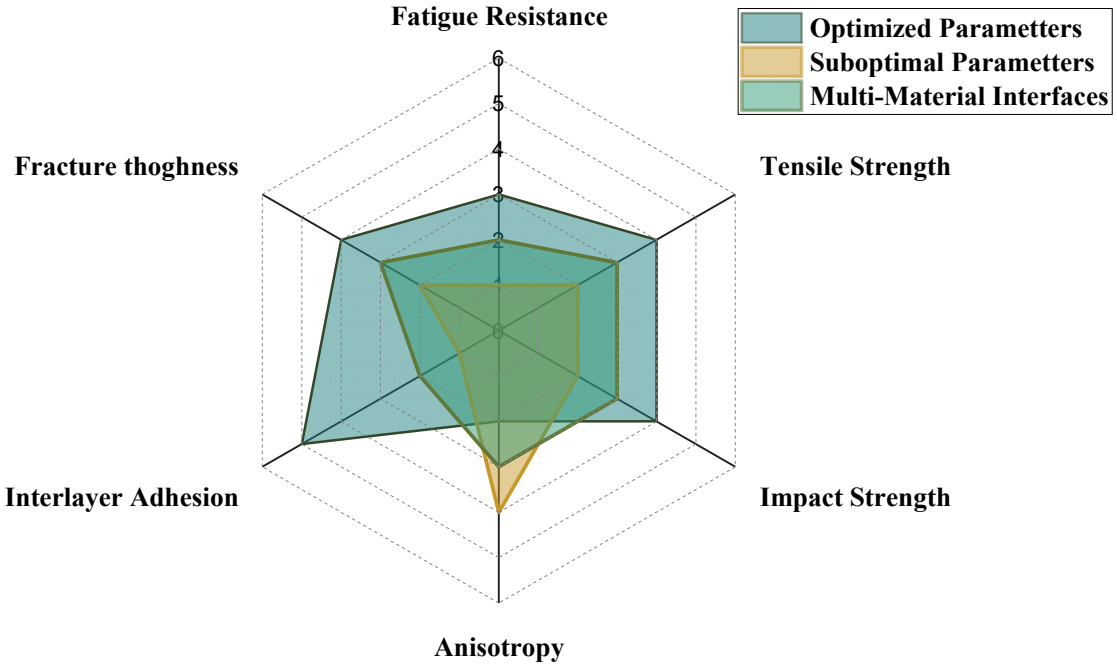

Figure 6: Relative mechanical performance of AM polymers under varying printing conditions, infill architectures, and material compositions [102].

Impact of infill geometry and density

The ability of modern AM to create highly customised interior architectures that create complex, strain fields of arbitrary and sometimes 3D serendipitous `materials' of extensible perspective interest is underpinned by recent works that exploit full-field optical techniques [88]. Hozdić and Hozdić [48] employed quantitative optical image analysis to determine a critical design tradeoff: linear infill patterns maximise tensile strength for neat PLA, whereas hexagonal patterns maximise ductility. For architected lattices, Popławski et al. [88] employed 3D-DIC to capture progressive deformation in hexagonal and re-entrant honeycombs, revealing a tendency to localise deformation to diagonal struts as compression progresses. Bolan et al. [15] linked energy absorption of octet-truss structures to relative density and strut geometry, finding that ductile resins have stable modes of collapse, while others yield catastrophic strut failure for high-strength variants. Bharat et al. [13] corroborated with a factorial ANOVA that infill density is the most important factor for compressive strength, accounting for >74% of variability for PLA-carbon fiber composites. Kumar et al. [57] found that for shape and lattice structures (rather than just solid geometries), a lower layer height (0.1 mm), as well as a higher infill of 100%, can improve flexural strength by reducing moulded-in stress concentrators. These experimental statements are inverted using inverse problem techniques. Wiklo et al. [110] found that coupling DIC with Finite Element Method Updating (FEMU) reveals that Young's modulus of PETG can vary up to 20% as a function of infill configuration. Guessasma et al. [43] extending on the work, used digital image correlation to derive finite element analysis (FEA) data for numerical material consumption on ABS, further explaining that build orientation effects overwhelm raster angle effects (35% drop vs. wire), and the use of numerical models essentially resolved macroscopic strain profiles as the result of filament dynamics.

Mesostructural defects and multi-material interfaces

Process-induced defects, related to voids (due to trapped air) and internal microcracks, are naturally linked to localised failure of 3D-printed polymers. Hozdić and Hozdić [48] found that pore morphology tends to correlate with tensile behaviour, using digital image processing (version 2.9.0) to show that densification tends to correlate with overall structural compactness, but micron-scale rule sets still govern pore (or generally defect) morphology. Similarly, Almeida Jr. et al. [7] used Time-Lapse Synchrotron X-ray CT to illustrate that the formation of voids develops predominantly at the ends of Fibres through a process of Strain-Incompatibility between the Rigid Carbon Fibres and the Yielding Nylon Matrix, which directly governs the Sequence of Ductile Fracture due to the Coalescence of Prolate-Ellipsoidal Voids (accounting for 2.3% of Volume) and Elongated Inter-Bead Channels, rather than Fibre Fracture. Corum et al. [20] discuss bead geometry and associated layer time with the «thinning effect» near bead edges that results from large-format AM, which considerably changes thermal expansion coefficients. Volumetric analysis via digital volume correlation (DVC) by Goyal et al. [41] also suggests that an increase in DVC data will yield an increase in internal displacement data visàvis infill percentage decrease due to slightly troughsize crosssections, and forms patterns of volumetric strain in craquelike «finger» patterns along rasters oriented at +45/−45 relative to the x-axis of the build surface. Mishra et al. [72] used SEM to show that the final density and hardness of PLA/wood dust composites were lessened through irregular bonding of the layers.

The introduction of secondary materials creates further interfaces that dictate the integrity of a structure. Ma et al. [65] combined AE-DIC-Micro-CT and detected the surface strain at which matrix cracking and fibre breakage of a 'sandwich' composite occurred. For sustainable manufacture, Bergaliyeva et al. [12] used DIC to identify the heterogeneous strain fields for virgin/recycled blend PLAs and examined how different extents of crystallinity and surface bonding gave rise to a loss in tensile properties. The risk of failure at chemically disparate interfaces from MM3DP (multi-material 3D printing) is well chronicled in the literature. Pahari et al. [78] demonstrate using the full-field DIC strain mapping technique that it is weak adhesion at boundaries that accounts for their integrated mechanical response. Maqsood and Rimašauskas [68] and Majid et al. [67] use DIC to expose mixed-mode paths of fracture and discontinuities in strain from cracking. To counter these failures, Nguyen et al. [77] developed dynamic covalent bonds within the printed networks that tend to undergo exchange reactions for repairing the layered material to a homogeneous network. For functionally graded systems, Popławski et al. [88] used 3D-DIC to validate the material model SAMP-1 for collapse behaviour of architected photopolymers, and Xu et al. [111] and Tang et al. [101] used DIC to investigate flexural mechanics and crack evolution of a cementitious composite reinforced with 3d printed polymer lattices.

Fracture mechanics and damage quantification

As the functionalities of AM go beyond the realm of prototyping and find utility as a functional end use, the layer-wise methodology of printing with polymers, along with the associated voids and anisotropy from thermal history, would continue to dictate macroscopic failure modes [90].

Real-time monitoring and crack path tracking

DIC continues to be crucial to visualising this evolution of the fracture, providing full-field mapping of displacements without the spatial constraints of traditional extensometers. Cracking in AM polymers is sensitive to the presence of defects internally, typically initiating at defects deep to the surface and propagating along weak interfacial paths between layers [6,96]. The observed trajectories can be significantly different from the expected behaviour as a result of anisotropy in the build orientation adopted [22,43]. In this sense, the trajectory is determined completely by print architecture. Isaac et al. [50] used DIC to show a reduction in the ability to sustain crack growth across [0/45/90/−45]n layups compared to 'baseline' rectilinear patterns. Automated analysis of DIC output has become prevalent. Gehri et al. [38] present a technique to skeletonize cracks represented as integrated lines to 0.02 mm, allowing for kinematic measures to be performed irrespective of crack orientation. Rahman et al. [90] adopt the SMART scheme in Ansys for modelling crack propagation, both static and fatigue (given that they find that crack propagation occurs sooner than with an unnotched specimen). More sophisticated treatments are possible. Shortly, Du et al. [27] describe the Radial Basis Point Interpolation Method (RPIM) for DIC data, to extract a smooth strain field (in those produced from noisy DIC data) to map the plastic region around crack tips. Crucially, these methods are allowing a better understanding of crack resistance and damage tolerance in complex printed geometries (Figure 7) as well as fracture surface features (Figure 8).

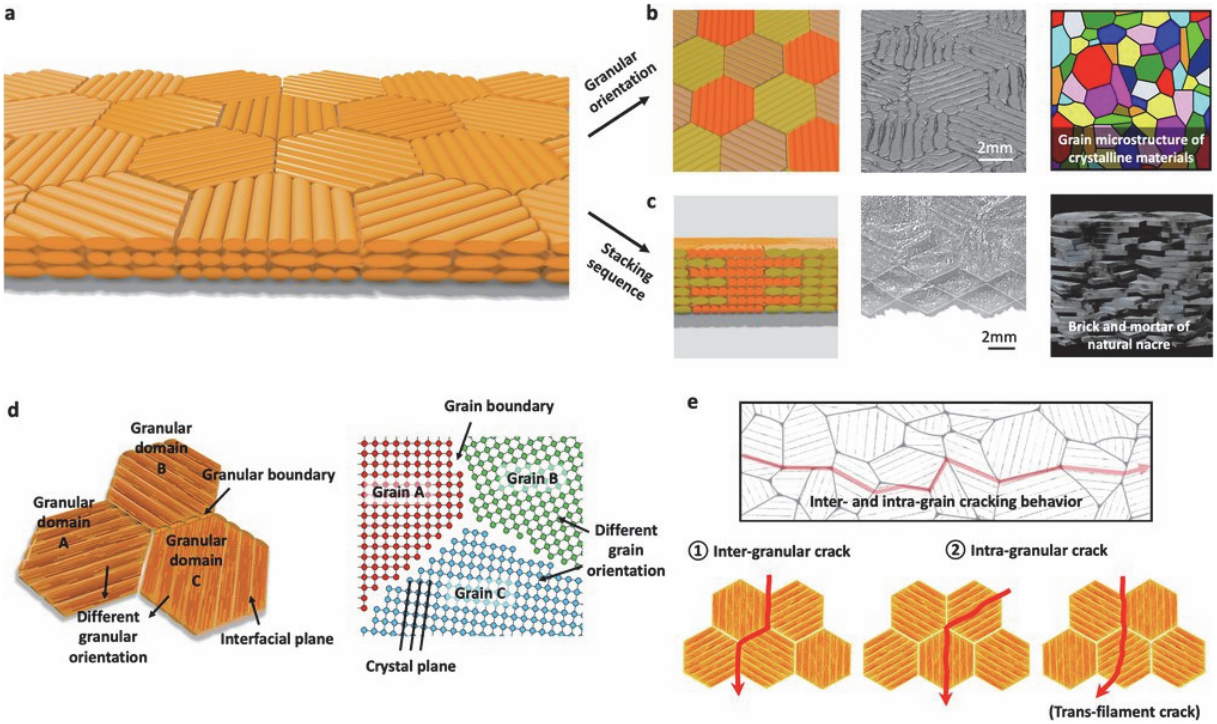

Figure 7: Example of a 3D-printed structure, where DIC can reveal crack resistance and damage tolerance.

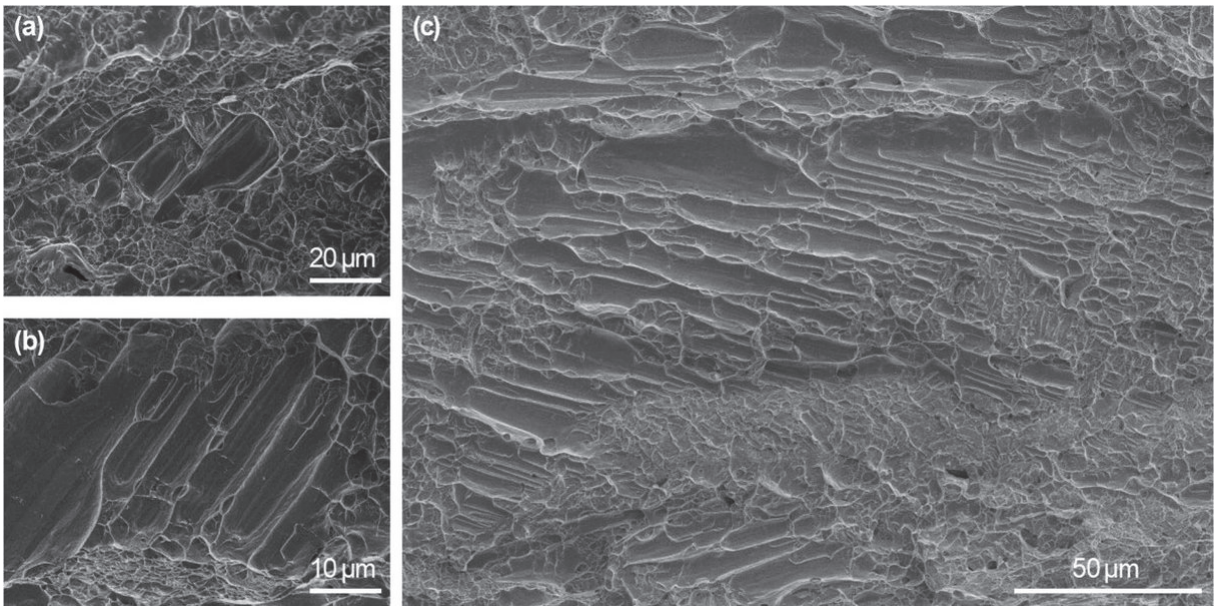

Figure 8: Example of a fracture surface showing typical features observed in additively manufactured materials.

Identification of fracture parameters (SIFs, CTOD, and J-Integral)

By resolving kinematic fields locally near a crack tip, specific measurements of interest, including Stress Intensity Factors (SIFs), Crack Tip Opening Displacement (CTOD), and the J-integral, can be extracted. DIC provides direct and accurate measurement of crack opening, primary to determining polymeric toughness, when subjected to cyclic loading. For complex anisotropic materials, Wang et al. [109] describe a methodology for orthotropic materials where experimentally determined elastic constants (E = 1.59 GPa, v = 0.28) are substituted into the plane strain modulus to determine E' = 1.7 GPa, leading to accurate predictions of fracture in layer structures. Franklinv and Christopher [35] describe how lightweight GPU-accelerated DIC enables the calculation of mixed-mode fracture parameters, exploiting the Benzeggagh-Kenane criterion to bridge the macro scale to material delamination and back through the extracted model parameters. Providing verifiable

feedback back into the digital twin, DIC is the lynchpin for enabling AM as a legitimate platform for safety-critical engineering [1]. A convenient mosaic of DIC-derived mechanical characterization, damage localization, and multimodal testing methodologies across all domains of loading is surveyed in Table 4.

Method / Application	Material(s)	Primary Findings	Key Insights & Practical Implications	Ref
Integrated DIC-FEMU	PET-G	Stiffness varies up to 20% based on infill pattern and density	Standard tensile tests oversimplify AM properties; full-field mapping is essential for precise constitutive modeling	[110]
Build Orientation Effects	PLA, Onyx, ABS	On-edge (YZ) orientation increases tensile strength by 19%; upright builds the weakest for axial loads.	Build orientation optimization can mitigate process-induced defects and extend component fatigue life.	[90,96]
Infill Geometry Optimization	PLA	Linear infill maximizes tensile strength; hexagonal patterns maximize ductility.	Critical design tradeoff between strength and ductility based on application requirements	[6,48]
Fracture & SMART Scheme	Onyx, ABS	Onyx exhibits higher fracture resistance than ABS; notched specimens fail prematurely.	FE modeling (SMART) validated by DIC provides a cost-effective path for structural certification.	[50,90]
Crack Path Tracking	PLA, ABS	[0/45/90/−45]n layups offer superior crack growth resistance vs. rectilinear patterns	Print architecture fundamentally governs crack trajectory and damage tolerance.	[27,50]
AE-DIC-Micro-CT Fusion	CCF-Sandwich	Damage categorized by frequency: Matrix (<50kHz), Debonding (50-150kHz), Fiber breakage (>150kHz)	Multi-modal NDT reveals progressive internal failure stages invisible to surface measurements alone.	[65]
Lattice Energy Absorption	Durable Resin, Acrylate	EA correlates linearly with strut radius; failure modes shift from layer-by-layer to catastrophic based on ductility.	Ductile resins preferable for stable shock absorption; SAMP-1 models accurately predict collapse mechanisms	[15,88]
AI-Assisted Crack Detection	CFRP, PLA	YOLOv5 and Deep DIC achieve >95% accuracy; TernausNet precision 0.819 vs 0.350 for thresholding	ML transforms raw DIC maps into intelligent diagnostic tools for high-throughput industrial QC.	[53,92,112]
Automated Crack Skeletonization	PLA, ABS	Morphological thinning detects 0.02 mm cracks (~0.05 pixels) with <0.008 mm uncertainty.	Direction-independent kinematic measurement outperforms conventional techniques by 1-2 orders of magnitude.	[38]
DIC-FBG Sensor Fusion	Concrete (transferable to AM)	Quasi-continuous crack tracking with high spatial resolution; correlates openings with strain reductions	Multimodal approach overcomes DIC's surface-only limitation and FBG's noise susceptibility.	[37]
Mixed-Mode Fracture (MMB)	Composites	GPU-accelerated DIC enables direct calculation of mixed-mode parameters via the Benzeggagh-Kenane criterion.	Bridges macroscopic deformation and microscale failure mechanisms (fiber pull-out, delamination)	[35]

Orthotropic Elastic Constants	Polymers (E=1.59 GPa, v=0.28)	Plane strain modulus calculations (E'=1.7 GPa) enable precise fracture prediction in layered AM structures.	Experimentally derived constants essential for accurate FE modeling of anisotropic AM parts	[109]
Environmental Coupling	PLA, Nylon	Mineral oil increases elongation by 76% (plasticization); moisture absorption degrades Nylon strength by 60%	Environmental resilience must be considered during the initial design of semi-lubricated or hygroscopic AM components	[57]
Layer Height Optimization	PLA	0.1 mm layer height with 100% infill significantly enhances flexural strength	Minimizing internal stress concentrators through process parameter control	[57]

Table 4: Mechanical Characterization and Damage Analysis in AM Polymers.

Advanced numerical extraction and optimization

Bolstering the accuracy of fracture parameters through a superior method of taking measurements:

- Meshless Refinement (RPIM): Du et al. [27] show RPIM is ~80% superior in convergence to conventional approaches, splitting the scales of continuous plastic deformations in high-gradient regions of crack tips.
- Numerical Synergy (SMART Scheme): Pairing DIC methods with adaptive remeshing within Ansys can provide greater economy in previously vexatious structural certification [90].
- High-Order Modeling: PP-4th order shape functions provide better measurement fidelity in complex, fractured lath structures inhomogeneous [89].
- Automated Crack Detection: Pipelines introduced in Gehri et al. [38] skeletonize a given crack, a propagating line uniquely, and track the locations of such closely, 0.02 mm (~0.05 pixels), allowing for objective kinematic measurements which are independent of path traversed.
- «Deep DIC» Robustness: The more contemporary DisplacementNet and StrainNet use a motion-capture style approach for attaining stable strain predictions. Apt in situations where torn speckles are produced by high ordering of polymer deformation [112].

ADVANCED FRONTIERS: AI, IN-SITU, AND MULTI-PHYSICS

The trajectory of DIC applications is gravitating away from post-build inspections toward real-time measurement of process, intelligent DIC-driven solvers, and multimodal sensor fusion. Extensible to a digital twin of the AM machine itself, real-time monitoring is essential for improving multi-material part adhesion and long-term thermomechanical robustness of polymers to environmental and dynamic loading [84]. DIC produces full-field experimental data, which are generally fed back to mechanical numerical solvers, facilitating design iteration and obviating the need for extensive physical prototyping.

Real-Time In-Situ monitoring and Digital Twin Integration

DIC transition from inspection toward active control of the AM represents a radical departure within AM quality assurance protocols. Fu et al. [36] developed a simulation-in-the-loop framework enabling real-time structural validation and a digital twin population that predictively models defects as they are created in fabrication, according to Figure 9. Intelligent DIC monitoring aspires to exceed passive sensing, with intelligent DIC being integrated with a control mechanism in the loop. Lu et al. [62] proposed a framework with deep learning and continual model-based validation for continuous fibre-reinforced composite, being a method learning to adapt the print parameters such that defects do not follow through the process. In FFF processes, Cunha et al. [22] highlight the implementation of 3DDIC in vacuum casing parts to help quantify the correlation between the layer-adhesion and microstructure defects. DIC enables robust in-process protocols for quality assurance. By identifying relationship with residual stresses and thermal deformations from the layer solidation process, DIC locates 'sweet spot' printing regimes to mitigate warping and excess stress entrapment, and Mejia et al. [69] evidences real time optical sensing in direct write of frontally polymerizing thermosets and presents the potential for autonomous decision support in manufacturing with DIC as a central tool of characterisation and intelligent health monitoring, aligning with the growing demand for responsive, smart manufacturing ecosystems as synthesized in Table 5.

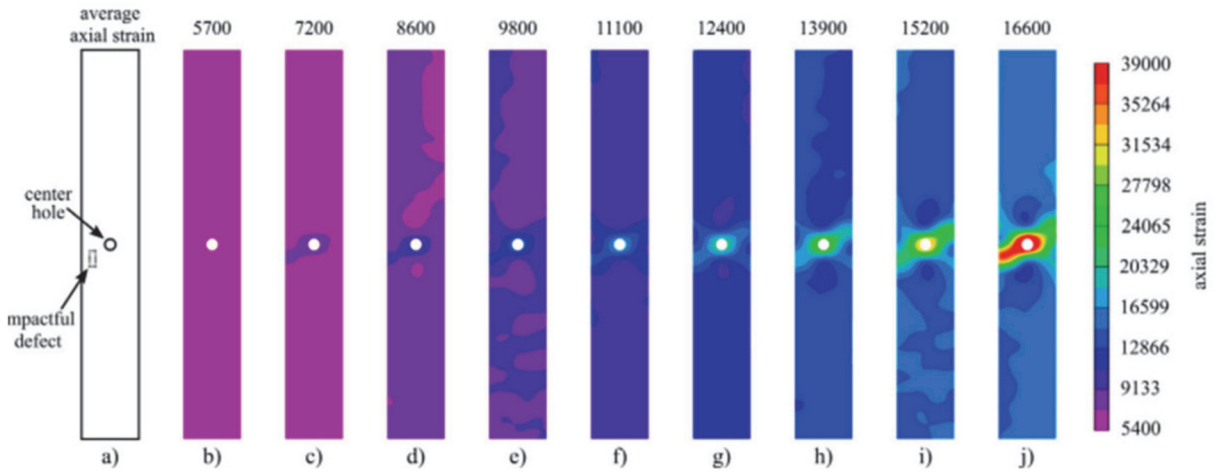

Figure 8: Strain distribution progression in a sample with an internal defect subjected to tensile loading [28].

Application Domain	Method / Technology	Main Findings	Key Insights & Practical Implications	Ref
In-situ Monitoring	Simulation-in-the-loop & Deep Learning	Enabled real-time defect detection and closed-loop process adjustment.	Transition from «as-designed» to «as-built» quality control reduces material waste and rework.	[36,62]
Process Validation	3D-DIC Topology Extraction	Quantifies relationships between building irregularities and microstructural defects.	Robust framework for in-process quality assurance; minimizes warping and residual stress.	[22,79]
Multi-material Interfaces	Full-field DIC Strain Mapping	Strain discontinuities at polymer interfaces (e.g., PLA-ABS) act as precursors to delamination.	Interface adhesion is the dominant failure driver; it necessitates optimized deposition sequences.	[68,78]
Recycled Blends	DIC Strain Heterogeneity Mapping	Increased recycled content leads to heterogeneous strain fields due to crystallinity variations.	DIC correlates processing-induced morphology changes with mechanical performance loss.	[12]
Architected Lattices	3D-DIC & SAMP-1 Modeling	Strain localizes on diagonal struts; energy absorption scales with relative density.	Scaled unit-cell testing allows for precise validation of nonlinear collapse models in complex geometries.	[15,88]
High-Speed Impact	Ultrahigh-speed DIC (UHS-DIC)	Resolves rapid strut buckling and plastic hinge formation in energy absorbers.	Standard static tests fail to capture rate-dependent failure modes essential for protective equipment.	[10]
Fatigue Analysis	Cyclic DIC Strain Mapping	Tracks crack initiation sites and propagation rates under repetitive stress.	Vital for assessing long-term reliability and predicting fatigue life of AM parts.	[115]
Environmental Coupling	DIC in Thermal/Humidity Chambers	Mineral oil increases elongation by 76% (plasticization); moisture degrades Nylon strength.	Environmental exposure significantly alters the «weld» quality between filaments, affecting long-term durability.	[48]
Structural Health Monitoring	DIC + Sensor Networks	Real-time strain mapping enables early damage detection and proactive maintenance.	Positions DIC at the nexus of material characterization and intelligent health monitoring.	[63,117]

Digital Twin Development	AE-DIC-FEA Integration	Real-time sensor feedback provides a complete picture of damage evolution.	Holistic NDE frameworks are the prerequisite for certifying AM components in safety-critical industries.	[36]

Table 4: In-situ Monitoring and Emerging DIC Applications in AM.

Artificial intelligence and «Deep DIC» architectures

Currently, the computational foundation of DIC technology is undergoing a paradigm shift away from traditional iterative sub-pixel methods of registration to a focus on developing deep learning-based neural networks (Deep DIC) that phase out the traditionally viewed amplification of noise. The end-to-end deep learning architecture developed by Yang et al. [112] (DisplacementNet and StrainNet) allows for consistent and robust accuracy in predicting strain across significant changes in speckle pattern distortion and the polymer deformation after a given load. Zhou et al. [118] recognized the critical limitation of DIC's ability to generalize to other scales and, therefore, created DICNO. DICNO utilizes neural operators to map latent image features directly onto a continuous field of displacement and offers vastly improved speed of inferences for different resolutions. MLF-DICNet, created by Yuan et al. [113] provides an automated means of developing all the multi-level feature fusion tensors, resulting in a reduction of the average absolute error when compared with traditional iterative DIC methods by 36.9% when applied to in-situ industrial environments. Utilizing transformer-based architectures (DICTr), Zhou et al. [119] utilized Transformer-based architectures (DICTr) to balance spatial resolution and accuracy in complex deformation fields. Lei et al. [58] coupled these models with attention mechanisms (AT-DICNet) to provide two-dimensional spatial resolution and accuracy in the complex deformation fields of polymeric structures to the micron level. Sadeghian et al. [93] emphasized the speed with which these DIC models, when combined with traditional optical analysis techniques via DIC, can transform pixel data into meaningful diagnostic outputs. Thus, damage detection and identifying engineering polymer materials can be executed in record time.

High-speed dynamics and automated damage tracking

In characterizing the impact resistance and fatigue crack propagation, both temporal and spatial frame rates are required that exceed the limits of conventional frame rate analysis. Comprehensive reviews of ultrahigh-speed DIC (UHS-DIC) by Arrington et al. [10] demonstrated its critical value in understanding the physical performance of ballistic response and dynamic failure modes of architected and engineered energy absorbers. Popławski et al. [88] showed that using high-speed image acquisition techniques on polymeric lattices could identify the transition phases occurring between stable buckling of struts and complete catastrophic failure based on the ratio of resin viscoelasticity to their relative density. To automate the quantification of cracks, Gehri et al. [38] developed the algorithm Morphological Thinning Pipeline, allowing for skeletonization of the cracks produced by a material or structure with a 0.02 mm accuracy (~0.05 pixels), thus providing directional-independent kinematic tracking of the cracks during their propagation. By utilizing TernausNet for deep learning-assisted crack segmentation, Rezaie et al. [92] surpassed traditional (threshold-based) segmentation techniques by producing segmentation results with a Precision of 0.819 vs 0.350. Similarly, Ke et al. [53] incorporated YOLOv5 frameworks into defect detection systems, enabling detection of objects in near real-time with a detection rate greater than 95%. The application of these automated systems significantly improves fatigue analysis capabilities, as demonstrated by Zappino et al. [114] who assessed the performance of cyclic DIC Strain Mapping to monitor the crack initiation locations and rate of crack propagation under variable amplitude loading conditions, providing essential input data for Paris Law modelling methods and Lifetime Predictions.

Environmental coupling and multiphysics characterization

The long-term service and performance of AM Polymers are heavily dependent on environmental service conditions, which necessitate a multiphysics approach to characterizing these materials. Hozdić and Hozdić [48] used DIC to show that mineral engine oil serves as a powerful plasticiser for both PLA and PLA+CF composites, resulting in increased nominal strain values at break (~76%), coupled with a significant degradation of stiffness and interfacial weld quality. Additionally, the impact of hygroscopicity must also be considered. Hou and Panesar [47] illustrated that ingress of moisture into the carbon fibre reinforced polyamide matrix leads to changes in the dimensional stability of these materials over time, whereas Gong et al. [40] confirmed that moisture absorption during filament production adversely affects both mechanical performance and surface finish. Environmental resilience should be viewed as a primary design consideration. Głowacki et al. [39] tested the tensile degradation of FDM polymers when subjected to shock-varied Temperature and Humidity and concluded that environmental resilience is a major design consideration for FDM polymers. In addition to these studies, Fidan et al. [32] evaluated the effectiveness of different layer heights on the sliding wear resistance of FDM polymers, indicating that the use

of thinner layer heights positively affects the abrasion resistance of ABS and PLA. Going forward, it will be important to quantify all mechanical, thermal, and chemical degradation mechanisms that affect the mechanical properties of FDM-produced polymers to fully understand the process-structure-property relationships of these materials.

Multimodal sensor fusion and NDE 4.0 paradigms

To overcome the surface-only limitation of optical metrology, DIC is increasingly integrated with volumetric and acoustic sensing techniques. Ma et al. [65] pioneered an AE-DIC-Micro-CT fusion approach for sandwich composites, correlating surface strain hotspots with specific acoustic frequency bands: matrix cracking (<50 kHz), debonding (50–150 kHz), and fiber breakage (>150 kHz). This combination allows for the accurate classification of internal progressive failure stages that cannot be seen with traditional surface measurements, as demonstrated by García de la Yedra et al. [37]. Cavagnis et al. [18] also illustrated similar principles by combining DIC and Fiber Bragg Grating (FBG) sensors to create a near-continuous crack tracking system that allows for more reliable detection by mitigating the noise susceptibility found in the individual optical fibre elements, Franklinv and Christopher [35] integrated a GPU-accelerated DIC system into their mixed-mode bending test system to calculate parameters related to delamination through the Benzeggagh-Kenane failure criterion, whilst Wang et al. [109] created frameworks for the analysis of orthotropic materials, where the elastic constants derived from DIC are used for the calculation of the plane strain modulus.

For obstructed environments, Fayad et al. [30] developed path-integrated X-ray DIC (PI-DIC) for use in obstructed environments by reformulating the matching criteria in order to use synthetic reference images, allowing the tracking of displacements within high-temperature build chambers. The combination of these modalities within the NDE 4.0 framework provides an important vision-based sensor for digital twins using DIC. Abdollahi-Mamoudan et al. [1] and Xu et al. [111] highlight how the combination of DIC and YOLOv7 (you only look once version 7) with DeepLabv3+ enables autonomous real-time quantification of damage. Additionally, Fayad et al. [30] proposed the use of real-time DIC information to support sensitivity-based decisions to reduce the impact of noise on material model identification. The integration of optical metrology, volumetric imaging [41,103], and AI-based diagnostics creates a pathway to «zero-defect» manufacturing environments in which the structural integrity of products is certified simultaneously with their creation.

EXPERIMENTAL-NUMERICAL SYNERGY AND INVERSE PARAMETER IDENTIFICATION IN AM POLYMERS

The merging of high-fidelity experimental measurement with advanced computational simulation denotes the current maximum of structural qualification for additively manufactured (AM) polymers. The complex, process-dependent, constitutive behaviour of these polymers makes it impossible to accurately capture the localized state of stress from the layer-wise mesostructures using traditional analytical models. A recent study employing Digital Image Correlation (DIC) as the primary tool for the calibration and validation of numerical frameworks has begun to create «digital twins» for autonomous manufacturing environments. The innovative connection formed between high-fidelity measurement and computational simulation has facilitated the acceleration of design iterations and significantly reduced the dependence on numerous physical prototypes, as well as enhancing the ability to predict [84].

Inverse problem-solving via Finite Element Method Updating (FEMU)

An important advance in the characterization of Additively Manufactured (AM) polymers has been the transition from manual curve-fit to automated inverse identification processes. Wikło et al. [110] implemented a methodology for solving inverse problems that combines DIC with Finite Element Method Updating (FEMU) for the precise identification of material parameter values for PET-G structural components. Through iterative minimization of the difference between experimental full-field strain maps and Finite Element Method (FEM) simulations, an accurate identification of Young's modulus and Poisson's ratio has been achieved for the proposed method. The study demonstrated up to 20% variability in the effective stiffness of Fused Deposition Modelling (FDM) components based on specific filament infill patterns and density. This variability illustrates the inadequacy of traditional tensile testing of point-based data in order to characterise anisotropic material systems. The foundation of the work presented by Wikło et al. [110] builds on the previous studies performed by Zouaoui et al. [120], whereby filament orientations and air-gap volume fractions were integrated directly into numerical meshes, and rigorously validated based on distributional strain data obtained from DIC.

Homogenization strategies and constitutive modeling

To reduce the computational burden associated with simulating intricate geometries made using AM techniques, there has been an increase in the use of homogenization methods that rely on the data obtained from DIC testing. A diffusion-like array of homogeneous and heterogeneous material behaviour zones has been established. Dialami et al. [24] demonstrated

the ability to predict FFF (Fused Filament Fabrication) component mechanical properties using an experimental validation procedure by separating the component into three distinct areas: aligned filament area, cross filament area, and inner structures. In addition to this, Machado and Cardoso [66] proposed performance coefficients based on the application of Classical Lamination Theory (CLT), which provide a balance of mechanical responses versus the amount of raw material that is consumed in fabrication and resulted in less than 9% deviation from experimentally obtained elastic moduli. Guessasma et al. [43] extended these insights using DIC-guided FEA on ABS, confirming that build orientation dominates raster angle effects (causing a 35% strength loss) and successfully reconciling macroscopic strain patterns with filament-scale mechanics.

Advanced numerical treatment of strain fields

The extraction of accurate strain data from noisy displacement fields is a critical requirement for robust fracture analysis and model calibration. The use of the Radial Basis Function Interpolation Method (RPIM) as introduced by Du et al. [27] proved successful in extracting strain data from raw DIC data via FEA in increasing the computational efficiency by almost 80% compared to conventional techniques, whilst being quite insensitive to the noise of displacements. This procedure supports reliability-based displacement tracking methodologies [81] and also follows the trend of new adaptive algorithms that utilize the principle of spatial continuity to reduce miscalculations associated with the complex inhomogeneous deformation [49].

Focus Area	Main Findings	Strategic Insight & Future Potential	Ref
Inverse Identification	Combined DIC and FEMU to identify Young's modulus and Poisson's ratio.	Bypasses the inaccuracies of extensometers in heterogeneous FFF structures.	[110,120]
Constitutive Modeling	Validated homogenization models for aligned and crossed filament paths.	Enables large-scale structural simulation without modeling individual print roads.	[24,43]
Meshless Processing	RPIM improves strain field extraction efficiency by 80%.	Essential for resolving high-gradient plastic zones at crack tips.	[27,81]
Real-time Validation	Simulation-in-the-loop enabled real-time structural health prediction.	Moves manufacturing from «post-build inspection» to «active process control.»	[36,63]
Data-Driven Design	Deep learning accelerated the discovery of optimal multi-material distributions.	Reduces the design iteration cycle for complex architected metamaterials.	[79]
Lamination Theory	CLT-based coefficients balanced stiffness and material consumption.	Provides a standardized analytical tool for industrial lamination-based AM.	[66]
Error Mitigation	Self-adaptive subset strategies optimized accuracy without manual intervention.	Removes user expertise as a barrier to high-precision DIC measurement.	[49]

Table 6: Experimental-Numerical Synergy in AM-DIC Workflows.

Simulation-in-the-loop and data-driven design

Integration of simulations within the fabrication has been pioneered by Fu et al. [36], who created a framework for simulation-in-the-loop that uses DIC data to provide real-time validation of an "as-built" component geometry against the idealized digital models. As this simulation-in-the-loop is developed further, Deep Learning (DL) applications will continue to emerge. For example, Chen et al. [19] demonstrated the potential of real-time decision-making for digital twins using time series Neural Networks and Model Predictive Control to identify and correct manufacturing defects before they reach the produced product, while Lu et al. [63] created closed-loop frameworks for continuous fibre-reinforced composites for adjusting to unexpected changes.

The combination of machine learning (ML) and experimental characterization will continue to support the rapid development of high-performance metamaterials. Sadeghian et al. [93] reported that combining Digital Image Correlation (DIC) with ML took raw pixels generated by DIC and converted them into useful, intelligent diagnostic data. Similarly,

Mishra et al. [71] employed ML in conjunction with DIC to accurately predict the flexural properties of wood-based composites. Furthermore, Pahlavani et al. [79] used deep learning based on computational simulations to rapidly develop the optimal distribution of materials for extremely unique mechanical properties like double-auxeticity. Table 6 provides a summary of the combination of DIC experiments with finite element modelling (FEM) and data-driven design.

MULTIMODAL NON-DESTRUCTIVE EVALUATION (NDE) AND VOLUMETRIC CHARACTERIZATION

Synergy of surface DIC and acoustic emission for damage categorization

When combining DIC with Acoustic Emission (AE) monitoring, an effective approach for tracking progressive damage to 3D printed composites is created. García de la Yedra et al. [37] presented evidence that surface-level strain measurement by DIC for predicting the initiation of internal delamination occurs considerably earlier than macroscopic failure in sandwich structures. In continuing with this dual-sensor approach, Ma et al. [65] combined DIC with AE and MicroCT to identify three types of bending-induced damage: Matrix cracking (<50kHz), Debonding (50-150kHz), and Fiber breakage (>150kHz). Additionally, Sadeghian et al. [93] emphasize that training machine learning algorithms on these coupled datasets transforms raw optical and acoustic signals into intelligent diagnostic tools for real-time structural health monitoring.

Volumetric strain analysis via Digital Volume Correlation (DVC)

Digital Volume Correlation (DVC) has arisen as the go-to method for mapping out 3D strain fields internally, overcoming the line-of-sight restriction inherent in surface DIC. Timpano and Melenka [103], for example, pioneered the application of an iterative Fast Iterative Digital Volume Correlation (FIDVC) algorithm to PLA-copper composites. They made the important finding that longitudinal strain development is "coupled" to the actual toolpath architecture internally, and not just in shell format on the surface outside. Goyal et al. [41] further identified that high volumetric strains mainly occur at the +45° and −45° raster orientations for high content FFF components, and the degree of internal displacement increases significantly with decreasing infill % due to the reduced cross-section able to bear loads. This information cannot be gained with surface DIC analysis alone, which only focuses on total displacement. Thus, this methodology sheds light on the challenging task of reconstructing complex crack fronts along with internal deformation in complex AM geometries.

Comparative analysis: DIC vs. OCT and X-ray computed tomography

Choosing the correct method for characterisation can often be about speeding up and downsampling, given the requirements of an AM polymer part. Kastner et al. [52] compare the performance of Optical Coherence Tomography (OCT) and X-ray Micro-Computed Tomography (μ-CT) on polymer composites. μ-CT provides volumetric imaging in 3D and, with the benefit of depth (though costly in operation), imaging at high resolution, though it is more expensive to operate and takes much longer to scan. OCT can also obtain quality cross-sectional micrometre-scale imaging, suitable for defect detection in translucent materials, and remarkable rapidity, but it cannot "see" very deep into a material. Abdollahi-Mamoudan et al. [1] advocate greater DIC capture of dynamic surface response under operational loading. Radiographic methods may be used to compare with the deformation mapping results from DIC. Note that absolute DIC knows nothing of how the damage it sees as the localised zones of higher strain actually manifests inside.

Advanced NDE 4.0 and Intelligent Data Fusion

By integrating DIC within the NDE 4.0 concept, structural life cycle management is transitioned from post-process inspection back to live, digital twin-enabled and IoT-supported autonomous diagnostics. Xu et al. [111] embedded DIC within YOLOv7 and DeepLabv3+ architectures to realise near real-time tracking of crack growth, achieving >95% accuracy, converting bare strain map data into automatic diagnostic outputs that effectively liberate operators from visual inspection fatigue. For noisy environments in which optical access is also foreclosed (such as high-temperature build chambers), Fayad et al. [30] realised a path-integrated X-ray DIC (PI-DIC) algorithm utilising synthetic reference images to successfully measure displacement of independently traced, moving internal layers. In addition to the identification of structural condition per se, Fayad et al. [29] generate a sensitivity-based decision process slate that guides the adjustment of noise influence across the inverse material parameter identification process via real-time DIC feedback. Both directly feed into «physics-informed» autonomous metrology that envisions a zero-defect manufacturing paradigm wherein structural health is ascribed in real-time without further human-in-the-loop stepping (see also Table 7 as benchmark).

Focus Area	Integrated DIC Method / Technology	Main Findings & Comparative Insights	Key Insights for AM Certification	Ref
Damage Categorization	AE-DIC-Micro-CT Fusion	Correlated surface strain hotspots with AE frequency bands (<50kHz for matrix, >150kHz for fiber).	Essential for verifying multi-stage failure in safety-critical AM components.	[37,65]
Volumetric 3D Strain	FIDVC (DVC)	Resolved internal 3D strain tensors; identified strain development along internal raster angles.	Moves characterization from surface-level estimation to true 3D «as-built» validation.	[41,103]
Metrological Performance	OCT vs. μ-CT Comparison	OCT offers lower cost and in-line suitability for translucent polymers; μ-CT remains the gold standard for depth.	Standardized protocols must define which technique is required based on material opacity and depth.	[52]
Internal Patterning	DVC on FFF Structures	Established that internal displacement fields are inherently coupled to toolpath architecture and infill density.	Validates the need for toolpath-aware numerical models in high-performance polymers.	[16,41]
Intelligent Diagnostics	DL-DIC Integration (YOLOv7)	Achieved near real-time crack tracking with >95% accuracy; transformed raw maps into diagnostic data.	Facilitates high-throughput industrial quality control for automated AM production lines.	[111]
Obstructed Environments	Path-Integrated X-ray DIC	Accurately measured independent displacement of multi-layered plates using synthetic reference images.	Opens new possibilities for testing AM parts within high-temperature build chambers or closed housings.	[30]
Hybrid Structure NDE	Optical-Radiographic NDE 4.0	Positioned DIC as a passive observer of surface strain hotspots caused by subsurface damage.	Integration of DIC with digital twins is the prerequisite for «zero-defect» manufacturing environments.	[1]

Table 7: Multimodal NDE Integration and Comparative DIC Analysis.

TECHNICAL EVOLUTION OF DIC: ADVANCED ALGORITHMS, METROLOGICAL STANDARDS, AND ALGORITHMIC INTELLIGENCE

Just as additive manufacturing (AM) aims to converge on production quality parameters aimed at high-performance components, the technical metrology core of Digital Image Correlation (DIC) has at last fully pivoted away from underlying traditional robustness in iterative matching towards a metrologically-aware intelligent and self-adaptive solver amenities. Particularly to address the interpolation associated with 3D-printed polymers, random behaviour fragments and complex surface topologies [63,79].

Metrological efficiency and boundary optimization

Arguments on DIC accuracy should be in context subset dimensions, where the spatial resolution increases with the size of the subset [91]. To remove the bias of manual parameters, Li et al. [59] proposed feature-based adaptive subset configurations, where geometry is optimized at each point of interest dynamically, allowing inhomogeneous fields of deformation to be accurately captured. To augment this, Su and Lao [98] developed mathematical frameworks of one-dimensional boundary subsets, which explicitly define the effects of invalid pixels in the specimen edges or crack paths on the accuracy of measurements, and thus improve the fidelity of fractured AM components.

Dynamic characterization and neural operator frameworks

Characterization of the microsecond scale. The effect characterization of polymeric lattices requires that the measurement scale be on the order of microseconds. Arrington et al. [10] critically examined the progress of ultrahigh-speed DIC (UHS-DIC), arguing that a standardized reporting procedure is essential to document rate-dependent failure modes across international sites. At the same time, machine learning has shifted DIC to data-driven, intelligent solvers, rather than iterative sub-pixel registration. Multi-level feature fusion (MLF-DICNet). Yuan et al. [113] minimized the mean absolute error by 36.9%, and DICNO by Zhou et al. [118] is a neural operator that scales and generalizes the solution by directly mapping the latent image features to continuous displacement fields. Zhou et al. [119] used Transformer architectures (DICTr) to trade off between spatial resolution and accuracy in complicated deformation patterns, Lei et al. [58] included attention mechanisms (AT-DICNet) to capture micron-level gradients, and Wang et al. [107] used displacement-field decomposition (StrainNet-LD) to retain fidelity in extreme speck.

Open-source ecosystems and algorithmic validation

Open-source platforms are robust and accelerate the democratization of DIC. Blaber et al. [14] and Turner et al. [105] defined foundational tools such as Ncorr and DICe, whereas Kibrete et al. [55] showed how current Python-based libraries can be used to integrate algorithms into experiment mechanisms quickly. Ahmad et al. [3] further support the idea of standardization through the use of Stereo-DIC Challenge 1.0 to test 3D-DIC performance under the rigid-body motion of complex, non-planar AM geometries. These metrological and algorithmic innovations are combined in Table 8, as part of a larger trend toward accuracy, automation, and accessibility of next-generation DIC workflows.

Technical Domain	Core Algorithmic / Procedural Advancement	Key Metrological Impact & Insight	Ref
Metrological Benchmarking	Established Metrological Efficiency Indicator (MEI) through Challenge 2.0.	Standardized the quantification of the noise-resolution trade-off in 2D DIC analyses.	[91]
Self-Adaptive Solvers	Developed feature-guided self-adaptive subset configuration.	Dynamically optimizes subset size/shape; removes user expertise as a bottleneck.	[59]
Dynamic Characterization	Reviewed High-Speed (HS) and Ultrahigh-Speed (UHS) DIC advancements.	UHS-DIC is essential for certifying rate-dependent failure in architected polymers.	[10]
Deep Learning Solvers	Introduced MLF-DICNet for multi-level feature fusion.	Reduced displacement measurement error by 36.9% compared to traditional DIC.	[107,113]
Complex Geometry	Hosted Stereo-DIC Challenge 1.0 for complex-shaped bodies.	Validated the ability of stereo-DIC to handle rigid body motion on non-planar surfaces.	[3]
Open-Source Tools	Evaluated Python-based open-source DIC ecosystems.	Facilitates global collaboration and rapid algorithmic deployment in research.	[14,55]
Edge Metrology	Developed accuracy models for one-dimensional boundary subsets.	Critical for accurately resolving strain at the edges of print layers or crack paths.	[98]

Table 8: Advanced DIC Techniques and Metrological Advancements.

HIGH-FIDELITY METROLOGY AND STANDARDIZATION PROTOCOLS FOR INDUSTRIAL AM-DIC INTEGRATION

Rigid metrological guidelines and standardized quantification of uncertainty. are needed to enable the transfer of DIC out of research into an industrial level of quality assurance in additive manufacturing. Metrological Efficiency Indicator (MEI) was developed by Reu et al. [91] through DIC Challenge 2.0, which serves as a definitive noise-resolution trade-off metric, making sure that filament-level strain peaks are observed without over-filtering. In conjunction with this, Beck [11] modeled noise propagation using virtual strain gauge (VSG) formulations, showed that the uncertainty of strain decays exponentially with the size of the VSG, and Grédiac et al. [42] used localized spectrum analysis to model camera sensor noise propagation to pre-calculate hardware sensitivity. Boundary subset accuracy models were further developed by Su and Lao [98] are important to maintain metrological fidelity to the sharp geometric edges of printed layers.

Industrial certification requires a high level of observance of traceable quality management systems. Measurement Management Systems outlined in ISO 10012:2026 are more and more used to regulate optical metrology in the production sector, and the iDICs Good Practices Guide (GPG) [51] mandates the use of calibration scoring and VSG reporting to combine the academic research and industry responsibility. Special data pipelines are necessary as scaling to high-resolution microscopy and large structural components is done. The PYVALE engine was demonstrated to scale to gigapixels of SEM image processing in Pureza et al. [89] and Venter and Neaves [106] and extended open-source scalability to high-order solutions using Julia and extensible Python frameworks was benchmarked against DIC Challenge 2.0. These pipelines can be used to quickly incorporate custom AM-specific failure criteria, based on underlying open-source frameworks such as Ncorr and DICe [14,105] and multi-scale prediction fusion networks [113,119] without compromising computational performance.

The combination of metrological rigor and AI-based diagnostics allows autonomous quality control. Computer vision and DIC were combined by Xu et al. [111] to reach more than 95% accuracy in real-time tracking of cracks, enabling real-time strain maps to be converted into traceable diagnostic results to certify a hybrid structure. Fayad et al. [29] have also proposed sensitivity-based decision making that reduces the effects of random noise when identifying the inverse parameters. This change of physics-inspired autonomous metrology forms a basis of standardized, auditable DIC processes, whereby AM parts are certified simultaneously with fabrication under internationally accepted reporting standards.

MULTI-MATERIAL INTERFACES, SUSTAINABLE POLYMER BLENDS, AND TRIBOLOGICAL PERFORMANCE CHARACTERIZED VIA DIC

Making additive manufacturing (AM) diversified toward functional uses necessitates an in-depth knowledge of how the configurations of complex materials respond to mechanical and environmental stressors in the real world. Digital Image Correlation (DIC) integration has become the key to the elimination of the distance between the theoretical material design and the real structural performance. Recent research has increased the usefulness of DIC to measure the impacts of the recycling cycles, lubricant exposure, and interfacial adhesion on the mechanical integrity of 3D-printed polymers.

Mechanical response of sustainable and reversible polymer networks

The shift to sustainable additive manufacturing has motivated the widespread study of upcycled polymers and self-healing networks, in which DIC is a key validation instrument to establish microstructure-to-property connections. Aly et al. [8] used DIC in conjunction with universal testing to compare virgin and recycled PLA blends, and found that DIC is sensitive to how the microscopic geometric defects of each single-screw extrusion relate to non-uniform strain patterns on the macroscopic load surface. This is consistent with that of Bergaliyeva et al. [12], who traced the heterogeneous strain fields in recycled PLA blends, and directly linked the changes in crystallinity and interfacial bonding to tensile performance degradation. To increase the stability of sustainable polymers, Nguyen et al. [77] considered dynamic covalent bonding approaches that facilitate the exchange reaction that converts a stratified layer network into more homogenous, self-healing structures. Piepoli et al. [87] also noted that sustainable feedstocks must be strictly optically characterized to certify their performance in unpredictable supply chains, making DIC a fundamental protocol that can validate recycled AM components.

Interfacial integrity and bond strength in multi-material systems

The structural reliability of multi-material 3D printing (MM3DP) is fundamentally constrained by chemical incompatibility and thermal mismatch at heterogeneous boundaries. Pahari et al. [78] utilized full-field DIC strain mapping across multi-material interfaces to identify weak adhesion zones as the primary drivers of premature structural failure, proving that DIC is indispensable for evaluating non-uniform load responses in anisotropic systems. In addition to this, Kumar et al. [56] were able to establish the first experimentally-based cohesive law definitions (τmax = 18.6 MPa and δc = 2.94 μm) for continuous fibre co-extrusion processes, which allow for the use of Physics-based Finite Element Modeling to study interfacial debonding in Additive Manufacturing printed composite materials. Maqsood and Rimašauskas [68] and Majid et al. [67] demonstrated that DIC resolves mixed-mode fracture paths at material junctions, quantifying strain discontinuities that serve as direct precursors to interfacial delamination. In specialized biomedical applications, Ki et al. [54] conducted a meta-analysis on the bond strength of 3D-printed resins for permanent restorations, highlighting that the printed-to-biological interface remains the most critical failure point. Minamino et al. [70] complemented this by using Optical Coherence Tomography (OCT) to reveal internal gaps between resin cores and dentin, providing a non-destructive

volumetric perspective that aligns with DIC's surface-level strain mapping. Furthermore, Dede et al. [23] established that preparation design in resin-based overlay restorations significantly impacts fit accuracy, requiring precise metrological verification during the digital design phase.

Tribological performance and environmental degradation

The long-term service life of AM polymers is heavily dictated by surface durability and environmental resilience under operational stressors. Fidan et al. [32] combined ANOVA and Scanning Electron Microscopy (SEM) to analyze sliding wear in ABS, PLA, and HIPS, revealing that thinner layer heights enhance wear resistance through increased surface homogeneity, with ABS exhibiting superior abrasion performance. Environmental exposure drastically alters these baseline properties; Hozdić and Hozdić [48] used DIC to monitor mineral engine oil coupling on PLA and PLA+CF composites, demonstrating that lubricant exposure acts as a potent plasticizer (increasing elongation by 76%) while simultaneously degrading interfacial weld quality and stiffness. Moisture ingress presents similar challenges: Gong et al. [40] confirmed that filament moisture absorption in Nylon directly correlates with reduced mechanical performance and surface degradation, while Hou and Panesar [47] quantified how hygroscopic expansion in carbon fiber-reinforced polyamides compromises dimensional stability over time. These findings establish environmental resilience as a primary design constraint for components intended for outdoor or semi-lubricated service environments.

Application / Material Focus	Integrated Methodology	Primary Findings & Insights	Strategic Impact for AM Technology	Ref
Sustainability & Recycling	DIC & Single-Screw Extrusion	Recycled/virgin PLA blends evaluated; DIC mapped strain distributions in filaments.	Validates upcycling viability; DIC identifies defects induced by recycling cycles.	[8,12]
Multi-material Interfaces	DIC & Shear Testing	Identified weak adhesion at MM3DP boundaries as the dominant failure driver.	Essential for predicting failure in customizable, heterogeneous structures.	[68,78]
Tribological Behavior	SEM, ANOVA & Wear Volume	Thinner layers improve wear resistance; ABS possesses superior abrasion resistance.	Informs parameter selection for components in sliding-contact applications.	[32]
Environmental Exposure	DIC & Mineral Oil Exposure	Lubricants act as plasticizers (76% elongation gain); micro-voids drive damage.	Crucial for designing AM parts for semi-lubricated or chemically harsh environments.	[40,48]
Structural Reinforcement	DIC & Concrete Elements	3D-printed PLA structures successfully reinforced concrete elements locally.	Provides sustainable, non-metallic alternatives for civil engineering projects.	[21,75]
Biomedical Restoration	Meta-analysis & Bond Strength	Quantified the critical interface strength of 3D-printed resins for restorations.	Standardizes certification requirements for additively manufactured medical implants.	[54,70]
Internal 3D Strain	DVC & Volumetric CT	Internal displacement fields coupled to the toolpath (+45/−45 raster angles).	Moves characterization from surface-level estimation to true 3D «as-built» validation.	[17,41]

Table 9: Sustainable Blends, Multi-material Interfaces, and Specialized Characterization.

Specialized case studies and multi-scale visualization

The application of DIC continues to expand into specialized civil engineering and nanoscale characterization domains. Csótár et al. [21] validated the use of 3D-printed PLA reinforcement structures in concrete elements, utilizing DIC to accurately capture crack arrest and load redistribution in sustainable non-metallic reinforcement. Németh et al. [75] extended this to railway sleepers, employing the GOM ARAMIS system to demonstrate how plastic fiber reinforcement significantly enhances crack resistance under cyclic bending loads. To bridge surface observations with internal phenomena, Bussey et al. [17] utilized X-ray nano-CT to visualize phase separation and porosity at 50 nm resolution, informing larger-scale DIC

models with nanoscale fracture initiation data. Goyal et al. [41] further established that internal displacement fields in metal-filled PLA are inherently coupled to raster orientations and infill density, with displacement increasing significantly as infill percentage decreases, a volumetric phenomenon that surface DIC alone cannot quantify. A comprehensive synthesis of these sustainable, multi-material, and specialized characterization workflows is provided in Table 9.

DEEP LEARNING ARCHITECTURES AND NEURAL OPERATORS: ADVANCED TECHNICAL REFINEMENTS

The transition toward autonomous AM certification requires DIC algorithms that dynamically adapt to heterogeneous surface topographies and quantify measurement uncertainty without manual intervention. Li et al. [59] developed a feature-guided self-adaptive subset configuration strategy that dynamically optimizes subset geometry at every point of interest, effectively capturing inhomogeneous deformation fields across complex 3D-printed surfaces. Complementing this, Su and Lao [98] established theoretical accuracy models for one-dimensional boundary subsets, explicitly characterizing how invalid pixels at specimen edges or crack paths influence measurement fidelity, a critical advancement for resolving strain concentrations at filament interfaces where failure initiates.

DIC Method / Architecture	Primary Foundational Technique	Main Findings & Metrological Insight	Strategic Impact for AM	Ref
DICNO (Neural Operator)	Latent feature mapping & multi-res training.	Achieved scale generalization and superior inference speed across datasets.	Enables «one-size-fits-all» solvers for multi-scale AM components.	[119]
MLF-DICNet	Encoder-decoder with multi-scale fusion.	MAE reduced by 36.9%; enabled mesoscopic in-situ measurement.	Optimized for real-time defect tracking in autonomous build environments.	[112,113]
Self-Adaptive Configuration	Feature-guided subset optimization.	Optimized subset parameters at POIs without user expertise.	Removes human bias; improves accuracy in heterogeneous AM strain fields.	[59]
VSG Uncertainty Models	Engineering error propagation.	Exponential decay of strain uncertainty relative to VSG size.	Provides the confidence bounds necessary for industrial certification.	[11,91]
DICLab2D (Julia)	High-order shape functions (up to 4th order).	Performance exceeds existing commercial codes for inhomogeneous fields.	High-performance open-source tools accelerate academic and SME innovation.	[89]
DICTr (Transformer)	Feature-matching via Transformer blocks.	Balanced spatial resolution and accuracy in complex patterns.	Robust correlation in low-contrast or distorted AM surfaces.	[119]
Boundary Subset Models	Edge-accuracy modeling.	Characterized influence of invalid pixels on boundary measurement fidelity.	Critical for strain mapping at the «neck» of filament interfaces.	[98]
SUN-DIC (Python)	Extensible open-source software.	Successfully benchmarked against DIC Challenge 2.0 datasets.	Facilitates rapid integration of custom AM-specific failure criteria.	[106]

Table 10: Technical Advancements in DIC Algorithmic Intelligence.

Rigorous uncertainty quantification remains foundational for industrial deployment. Beck [11] formalized noise propagation through Virtual Strain Gauge (VSG) formulations, demonstrating an exponential decay relationship between strain uncertainty and VSG size that provides mathematical confidence bounds for full-field maps. To enhance tracking stability over extended deformation cycles, Feng et al. [31] introduced a loosely coupled serial DIC framework, while Wang et al. [107] deployed StrainNet-LD, which utilizes displacement-field decomposition to maintain precision during extreme plastic flow and speckle distortion. These refinements are anchored by the standardized noise-resolution benchmarks established

in DIC Challenge 2.0 [91]. Collectively, these algorithmic innovations, neural operators, and open-source architectures are comprehensively benchmarked in Table 10.

CRITICAL DISCUSSION, METHODOLOGICAL LIMITATIONS, AND FUTURE PERSPECTIVES

The DIC is no longer a part of optical methods but is now a foundation metrology of measuring the complicated mechanical behavior of AM polymers. The major benefit of DIC is that it can clean up the full-field strain concentration at filament interfaces, interlayer voids, and crack propagation paths that determine the anisotropic failure of printed polymers. DIC unlike point-wise sensors captures localized strain gradients without mechanical interference and thus allows the validation of multi-scale constitutive models and the identification of inverse parameters using FEMU. Moreover, the combination of DIC with high-speed imaging, DVC, and multimodal NDE models (AE, μ-CT) led to a complete damage-tracking pipeline that has the capability to relate surface deformation with internal defect development. Nevertheless, there are a number of methodological limitations to be considered. To start with, DIC is always surface-based, and therefore, it does not reveal the coalescence of voids in the subsurface, or internal delamination unless used in conjunction with volumetric methods such as DVC or μ-CT, which are computationally intensive and necessitate specialized equipment. Second, the quality of speckles, the size of the subsets, and the topography of the surface are very sensitive to the measurement accuracy. Poor choice of subset may flatten high strain peaks between beads and the fracture parameters would be undervalued. Third, though Deep DIC and neural operators (DICNO, StrainNet-LD) are much less susceptible to noise amplification and faster than their counterparts, they have domain-shift weaknesses when used on AM surfaces with changing light illumination, translucency, or uncontrolled speckle degradation. Purely data-driven models, with no physics-informed constraints, are likely to generate non-physical strain fields. Three priorities can be identified to bring DIC to a step further in terms of academic validation and industrial certification. To start with, standardized metrological reporting should be brought into compulsory. The reproducibility and regulatory acceptance will be ensured with widespread usage of MEI, VSG uncertainty quantification, and iDICs Good Practices Guide. Second, hybrid metrology pipelines must be created to circumvent line-of-sight limitations and combine high-throughput 3D-DIC with radiographic inspection to targeted areas within NDE 4.0 paradigms. Third, the next-generation DIC algorithms should include physics-informed machine learning, which ensures thermodynamic consistency, strain compatibility, and fracture mechanics constraints to avoid non-physical predictions during extreme deformation. With AM geometries approaching micro-lattices and fine-resolution resins, Micro-DIC will be a necessary tool to measure individual-road strain distributions and check the interfacial diffusion models. Finally, through uncertainty reporting and multimodal sensing standardization and the integration of DIC into closed-loop digital twins, the method will become the crucial experimental interface that approves AM polymers to be used in safety-critical aerospace, biomedical, and automotive application.

CONCLUSION

This review systematically evaluated the transformative role of Digital Image Correlation (DIC) in characterizing the mechanical behavior and fracture mechanics of additively manufactured polymers. Conventional point-wise sensors consistently fail to capture the severe mechanical anisotropy, interlayer voids, and localized strain concentrations inherent to layer-wise fabrication. DIC overcomes these limitations by providing high-resolution, non-contact full-field measurements that reveal the exact progression of inter-bead strain localization, crack initiation, and anisotropic damage accumulation. Key findings demonstrate that build orientation, infill architecture, and thermal history dictate the structural reliability of printed polymers such as PLA, ABS, Onyx, and advanced composites. Digital image correlation (DIC) is an important tool for optimizing toolpath generation, validating multi-scaled constitutive models, and extracting reliable fracture parameters (SIF, CTOD, and J-integrals) for geometries produced from very complex processes. The continued development of DIC technology has allowed for the growth of capabilities from static two-dimensional mapping to dynamic high-speed (ultrahigh velocity) dynamic tracking, to stereo-DIC for non-planar surfaces, and volumetric DVC (Digital Volumetric Correlation) for the determination of internal strain. Deep DIC algorithms and neural operators have been developed, improving measurement accuracy by up 37% and enabling automated defect identification in real-time. In order for DIC to be accepted as a viable and trusted measurement method for regulatory compliance for safety critical industries, there needs to be a standard set of metrology protocols adopted universally. Implementation of the Metrological Efficiency Indicator (MEI), development and the use of accurate uncertainty quantification protocols, and compliance with the iDICs Good Practices Guide will eliminate inconsistencies in reporting and allow DIC to be used as a legally defensible method

of certifying the validity of measurements. DIC bridges the gap between as-designed simulations and as-built experimental validation by providing the critical feedback loop necessary for transforming additive manufacturing into a reliable, scalable solution for high-performance engineering applications. DIC will continue to converge with artificial intelligence, multimodal sensing, and PAC-Physics informed Digital Twins to enable the structural and functional integrity of additive manufactured polymer-based components in next-generation industrial systems.

ACKNOWLEDGMENTS

The authors thank Prof. Humberto Almeida Jr. (LUT University, Finland) for his comments and valuable feedback on earlier versions of this manuscript. His valuable suggestions on digital image correlation and additive manufacturing topics are discussed in this review.

NOMENCLATURE AND ABBREVIATIONS

AM:	Additive Manufacturing
DIC:	Digital Image Correlation
DVC:	Digital Volume Correlation
FFF:	Fused Filament Fabrication
SLA/DLP:	Stereolithography / Digital Light Processing
SLS:	Selective Laser Sintering
MEI:	Metrological Efficiency Indicator
ROI:	Region of Interest
ZNSSD:	Zero-mean Normalised Sum of Squared Differences
IC-GN:	Inverse Compositional Gauss–Newton
VSG:	Virtual Strain Gauge
FEMU:	Finite Element Method Updating
SIF:	Stress Intensity Factor
CTOD:	Crack Tip Opening Displacement
AE:	Acoustic Emission
μ-CT:	Micro-Computed Tomography
ML/DL:	Machine Learning / Deep Learning
NDE:	Non-Destructive Evaluation

REFERENCES

[1] Abdollahi-Mamoudan, F., Ibarra-Castanedo, C., Maldague, X.P.V. (2025). Non-Destructive Testing and Evaluation of Hybrid and Advanced Structures: A Comprehensive Review of Methods, Applications, and Emerging Trends, Sensors, 25(12). DOI: https://doi.org/10.3390/s25123635

[2] Acciaioli, A., Lionello, G., Baleani, M. (2018). Experimentally Achievable Accuracy Using a Digital Image Correlation Technique in measuring Small-Magnitude (<0.1%) Homogeneous Strain Fields, Materials, 11(5), p. 751. DOI: https://doi.org/10.3390/ma11050751

[3] Ahmad, W., Helm, J., Bossuyt, S., Reu, P., Turner, D., Luan, L K., Lava, P., Siebert, T., Simonsen, M., Fi, W.A., Helm, J., Bossuyt, S., Reu, P., Gov, P., Turner, D., Luan, L.K., Lava, P., Simonsen, M. (2024). Stereo-DIC Challenge 1.0 – Rigid Body Motion of a Complex Shape, Experimental Mechanics, 64(7), pp. 1073–1106. DOI: https://doi.org/10.1007/s11340-024-01077-7

[4] Albaşkara, M., Yıldız, İ. (2025). A comparative study on the tensile properties of PLA, PETG, and ABS in FDM 3D printing: effects of infill geometry and build orientation, International Journal of 3D Printing Technologies and Digital Industry, 9(3), pp. 688–697. DOI: https://doi.org/10.46519/ij3dptdi.1779348

[5] Alghamdi, S.S., John, S., Choudhury, N.R., Dutta, N.K. (2021). Additive Manufacturing of Polymer Materials: Progress, Promise and Challenges, Polymers (Basel)., 13(5), p. 753. DOI: https://doi.org/10.3390/polym13050753

[6] Ali, S., Abdallah, S., Devjani, D.H., John, J.S., Samad, W.A., Pervaiz, S. (2023). Effect of build parameters and strain rate on mechanical properties of 3D printed PLA using DIC and desirability function analysis, Rapid Prototyp. J., 29(1), pp. 92–111. DOI: https://doi.org/10.1108/RPJ-11-2021-0301
[7] Almeida, J.H.S., Miettinen, A., Léonard, F., Falzon, B.G., Withers, P.J. (2025). Microstructure and damage evolution in short carbon fibre 3D-printed composites during tensile straining, Compos. B Eng., 292, p. 112073. DOI: https://doi.org/10.1016/J.COMPOSITESB.2024.112073
[8] Aly, R., Olalere, O., Ryder, A., Alyammahi, M., Samad, W.A. (2024). Mechanical Property Characterization of Virgin and Recycled PLA Blends in Single-Screw Filament Extrusion for 3D Printing, Polymers, 16(24). DOI: https://doi.org/10.3390/polym16243569
[9] Armstrong, M., Mehrabi, H., Naveed, N. (2022). An overview of modern metal additive manufacturing technology, J. Manuf. Process., 84(12), pp. 1001–1029. DOI: https://doi.org/10.1016/j.jmapro.2022.10.060
[10] Arrington, A., Westra, A., Jannotti, P., Reu, P., Lamberson, L. (2025). Review of High-Speed Digital Image Correlation: Advancements and Good Practices, Strain, 61(6), p. e70018. DOI: https://doi.org/10.1111/str.70018
[11] Beck, P.M. (2025). Propagation of Noise Uncertainty Through Virtual Strain Gauge Formulations for 2D Digital Image Correlation, Experimental Techniques, pp. 1–9. DOI: https://doi.org/10.1007/s40799-025-00828-y
[12] Bergaliyeva, S., Sales, D.L., Delgado, F.J., Bolegenova, S., Molina, S.I. (2023). Manufacture and Characterization of Polylactic Acid Filaments Recycled from Real Waste for 3D Printing, Polymers, 15(9). DOI: https://doi.org/10.3390/polym15092165
[13] Bharat, N., Kumar, V., Mishra, V., Veeman, D., Vellaisamy, M. (2025). Influence of 3D Printing FDM Process Parameters on Compressive Strength of PLA/Carbon Fiber Composites: ANOVA and Backpropagation Neural Network Approach, Journal of Materials Engineering and Performance, 34(18), pp. 20830–20843. DOI: https://doi.org/10.1007/s11665-025-10783-9
[14] Blaber, J., Adair, B., Antoniou, A. (2015). Ncorr: Open-Source 2D Digital Image Correlation Matlab Software, Experimental Mechanics, 55(6), pp. 1105–1122. DOI: https://doi.org/10.1007/s11340-015-0009-1
[15] Dean, M., Bardelcik, A. (2023). The Energy Absorption Behavior of 3D-Printed Polymeric Octet-Truss Lattice Structures of Varying Strut Length and Radius, Polymers 15(3). DOI: https://doi.org/10.3390/polym15030713
[16] Buljac, A., Jailin, C., Mendoza, A., Neggers, J., Taillandier-Thomas, T., Bouterf, A., Smaniotto, B., Hild, F., Roux, S. (2018). Digital Volume Correlation: Review of Progress and Challenges, Exp. Mech., 58(5), pp. 661–708. DOI: https://doi.org/10.1007/s11340-018-0390-7
[17] Bussey, J.M., Weber, M.H., Smith-Gray, N.J., Sly, J.J., McCloy, J.S. (2023). Examining phase separation and crystallization in glasses with X-ray nano-computed tomography, J. Non. Cryst. Solids, 600(1), p. 121987. DOI: https://doi.org/10.1016/j.jnoncrysol.2022.121987
[18] Cavagnis, F., Fernández Ruiz, M., Muttoni, A. (2018). A mechanical model for failures in shear of members without transverse reinforcement based on development of a critical shear crack, Eng. Struct., 157, pp. 300–315. DOI: https://doi.org/10.1016/j.engstruct.2017.12.004
[19] Chen, Y.P., Karkaria, V., Tsai, Y.K., Rolark, F., Quispe, D., Gao, R.X., Cao, J., Chen, W. (2025). Real-time decision-making for Digital Twin in additive manufacturing with Model Predictive Control using time-series deep neural networks, J. Manuf. Syst., 80(6), pp. 412–424. DOI: https://doi.org/10.1016/j.jmsy.2025.03.009
[20] Corum, T.M., O'Connell, J.C., Pankratz, S., Heres, M., Foote, J., Duty, C.E. (2026). Effect of Bead Geometry and Layer Time on Microstructure and Thermomechanical Properties of Large-Format Polymer Composites, Polymers 18(1). DOI: https://doi.org/10.3390/polym18010133
[21] Csótár, H., Szívós, B.F., Szalai, S., Fischer, S. (2025). Production and Testing of 3D Printed PLA Structures with DIC Technology for the Reinforcement of Concrete Elements, Lecture Notes in Networks and Systems, 1258 LNNS, pp. 175–187. DOI: https://doi.org/10.1007/978-3-031-81799-1_17
[22] Cunha, F.G., Santos, T.G., Xavier, J. (2021). In Situ Monitoring of Additive Manufacturing Using Digital Image Correlation: A Review, Materials 14(6), p. 1511. DOI: https://doi.org/10.3390/MA14061511
[23] Dede, D.Ö., Zeller, D.K., Demirel, M., Al-Johani, H., Schimmel, M., Çakmak, G., Yilmaz, B., Donmez, M.B. (2025). Effect of manufacturing trinomial and preparation design on the fabrication and fit accuracy of additively and subtractively manufactured resin-based overlay restorations, J. Dent., 157(3), p. 105687. DOI: https://doi.org/10.1016/j.jdent.2025.105687
[24] Dialami, N., Rivet, I., Cervera, M., Chiumenti, M. (2023). Computational characterization of polymeric materials 3D-printed via fused filament fabrication, Mechanics of Advanced Materials and Structures, 30(7), pp. 1357–1367. DOI: https://doi.org/10.1080/15376494.2022.2032496

[25] Diani, J., Geraud, G., Coq, A., Kuzyara, V. (2026). Stamps for Pattern Applications for DIC or Markers Tracking, Experimental Techniques 2026, pp. 1–11. DOI: https://doi.org/10.1007/s40799-026-00875-z
[26] Dong, Y.L., Pan, B. (2017). A Review of Speckle Pattern Fabrication and Assessment for Digital Image Correlation, Exp. Mech., 57(8), pp. 1161–1181. DOI: https://doi.org/10.1007/S11340-017-0283-1
[27] Du, J., Zhao, J., Zhao, J., Zhao, J., Liu, J., Liu, J., Zhao, D., Zhao, D., Zhao, D. (2024). Radial basis point interpolation for strain field calculation in digital image correlation, Applied Optics, 63(14), pp. 3929–3943. DOI: https://doi.org/10.1364/ao.520232
[28] Enriconi, M., Rodriguez, R., Araújo, M., Rocha, J., García-Martín, R., Ribeiro, J., Pisonero, J., Rodríguez-Martín, M. (2025). A Comprehensive Review of Fused Filament Fabrication: Numerical Modeling Approaches and Emerging Trends, Applied Sciences, 15(12). DOI: https://doi.org/10.3390/app15126696
[29] Fayad, S.S., Jones, E.M.C., Seidl, D.T., Lambros, J. (2025). Identification Uncertainty in Inverse Material Model Parameter Determination: A Sensitivity-Based Decision Process for Load Path Selection, Strain, 61(3), p. e70007. DOI: https://doi.org/10.1111/str.70007
[30] Fayad, S.S., Jones, E.M.C., Winters, C. (2024). Path-Integrated X-Ray Digital Image Correlation using Synthetic Reference Images, Experimental Techniques 2024 48:6, 48(6), pp. 941–951. DOI: https://doi.org/10.1007/s40799-024-00707-y
[31] Feng, M., Yuan, X., Xiao, H., Mou, N., Huang, S. (2025). A loosely coupled serial digital image correlation method based on deep learning, Measurement (Lond), 253. DOI: https://doi.org/10.1016/j.measurement.2025.117783
[32] Fidan, S., Ürgün, S., Şahin, A.E., Bora, M.Ö., Yılmaz, T., Özsoy, M.İ. (2025). Comprehensive Sliding Wear Analysis of 3D-Printed ABS, PLA, and HIPS: ANOVA, SEM Examination, and Wear Volume Measurements with Varying Layer Thickness, Polymers (Basel)., 17(14). DOI: https://doi.org/10.3390/polym17141899
[33] Fisher, T., Almeida, J.H.S., Falzon, B.G., Kazancı, Z. (2023). Tension and Compression Properties of 3D-Printed Composites: Print Orientation and Strain Rate Effects, Polymers 15(7), p. 1708. DOI: https://doi.org/10.3390/POLYM15071708
[34] Fisher, T., Kazancı, Z., Almeida, J.H.S. (2024). The importance of print orientation in numerical modelling of 3D printed structures under impact loading, Mater. Res. Express, 11(6), p. 065303. DOI: https://doi.org/10.1088/2053-1591/AD59F1
[35] Franklinv, A., Christopher, T. (2019). Generation of mixed mode I/II failure criteria from MMB specimens: an experimental study, Mater. Res. Express, 6(12), p. 125616. DOI: https://doi.org/10.1088/2053-1591/ab5c8e
[36] Fu, Y., Downey, A.R.J., Yuan, L., Huang, H.T., Ogunniyi, E.A. (2025). Simulation-in-the-loop additive manufacturing for real-time structural validation and digital twin development, Addit. Manuf., 98, p. 104631. DOI: https://doi.org/10.1016/j.addma.2024.104631
[37] García de la Yedra, A., Erro, I., Vivas, J., Zubiri, O., Zurutuza, X., Sommerhuber, R., Kettner, M. (2024). Acoustic Emission and Digital Image Correlation-Based Study for Early Damage Identification in Sandwich Structures, Applied Sciences, 14(21). DOI: https://doi.org/10.3390/app14219728
[38] Gehri, N., Mata-Falcón, J., Kaufmann, W. (2020). Automated crack detection and measurement based on digital image correlation, Constr. Build. Mater., 256, p. 119383. DOI: https://doi.org/10.1016/J.CONBUILDMAT.2020.119383
[39] Głowacki, M., Skórczewska, K., Lewandowski, K., Szewczykowski, P., Mazurkiewicz, A. (2023). Effect of Shock-Variable Environmental Temperature and Humidity Conditions on 3D-Printed Polymers for Tensile Properties, Polymers 16(1). DOI: https://doi.org/10.3390/polym16010001
[40] Gong, H., Runzi, M., Wang, Z., Wu, L., Zhang, Y. (2025). Influence of Filament Moisture on 3D Printing Nylon, Technologies 13(8). DOI: https://doi.org/10.3390/technologies13080376
[41] Goyal, A., Timpano, C.S., Melenka, G.W. (2023). Mapping internal strain fields of fused filament fabrication metal filled polylactic acid structure using digital volume correlation, J. Compos. Mater., 57(14), pp. 2311–2324. DOI: https://doi.org/10.1177/00219983231171658
[42] Grédiac, M., Sur, F., Vinel, A., Jailin, T., Blaysat, B. (2025). Predicting Camera Sensor Noise Propagation to Displacement and Strain Maps Retrieved from Checkerboard Patterns with Localized Spectrum Analysis, Experimental Mechanics 65(8), pp. 1237–1257. DOI: https://doi.org/10.1007/s11340-025-01207-9
[43] Guessasma, S., Nouri, H., Belhabib, S. (2022). Digital Image Correlation and Finite Element Computation to Reveal Mechanical Anisotropy in 3D Printing of Polymers, Materials 15(23), p. 8382. DOI: https://doi.org/10.3390/MA15238382
[44] Hachimi, T., Ait Hmazi, F., Arhouni, F.E., Zekriti, N., Doghmi, H., Majid, F. (2026). Damage evolution and fracture behavior in 3D-printed materials: effects of crack propagation and progressive layer degradation, Progress in Additive Manufacturing, 11(3), pp. 2591–2610. DOI: https://doi.org/10.1007/S40964-025-01484-9

[45] Hachimi, T., Ait Hmazi, F., Majid, F. (2025). Damage of additively manufactured polymer materials: experimental and probabilistic analysis, Fracture and Structural Integrity, 19(73), pp. 236–255. DOI: https://doi.org/10.3221/IGF-ESIS.73.16
[46] Holzmond, O., Li, X. (2017). In situ real time defect detection of 3D printed parts, Addit. Manuf., 17, pp. 135–142. DOI: https://doi.org/10.1016/j.addma.2017.08.003
[47] Hou, Y., Panesar, A. (2025). The moisture absorption of additively manufactured short carbon fibre reinforced polyamide, Compos. Part A Appl. Sci. Manuf., 188(3), p. 108528. DOI: https://doi.org/10.1016/j.compositesa.2024.108528
[48] Hozdić, E., Hozdić, E. (2025). Mechanical Parameters and Microstructural Evolution of FDM-Printed PLA and PLA+CF Under Variable Infill Architecture and Lubricant Exposure, Polymers, 18(1). DOI: https://doi.org/10.3390/polym18010072
[49] Hu, J., Miao, H., Xu, J., Zhang, R., Lai, L., Deng, Y. (2025). Adaptive undermatched systematic error mitigation algorithm considering spatial continuity in digital image correlation, Surf. Topogr., 13(3), p. 035001. DOI: https://doi.org/10.1088/2051-672X/ade7a4
[50] Isaac, J.P., Dondeti, S., Tippur, H. V. (2020). Crack initiation and growth in additively printed ABS: Effect of print architecture studied using DIC, Addit. Manuf., 36, p. 101536. DOI: https://doi.org/10.1016/j.addma.2020.101536
[51] Jones, A., DiCecco, S., Furmanski, J., Harmon, B., Koohbor, B., Mathieu, F., Blaysat, B., Coret, M., Hild, F., Lava, P., Passieux, J.-C., Périé, J.-N., Réthoré, J., Swiergiel, N., Tong, Z., Yang, J. (2025). A Good Practices Guide for Digital Image Correlation. DOI: https://doi.org/10.32720/idics/gpg.ed2
[52] Kastner, J., Schlotthauer, E., Burgholzer, P., Stifter, D. (2004). Comparison of x-ray computed tomography and optical coherence tomography for characterisation of glass-fibre polymer matrix composites., Proceedings of World Conference on Non Destructive Testing, pp. 71–79.
[53] Ke, Y., Han, C., Sun, B., Wu, X. (2025). Failure analysis and on-line damage monitoring based on deep-learning for thermo-oxidative aged 3D angle-interlock woven composites under tension, Eng. Fail. Anal., 174, p. 109484. DOI: https://doi.org/10.1016/j.engfailanal.2025.109484
[54] Ki, M., Hayashi, M., Kim, M. (2025). 3D-printed resin for permanent/definitive restorations: meta-analysis for bond strength, PeerJ Materials Science, 7, p. e35. DOI: https://doi.org/10.7717/peerj-matsci.35
[55] Kibrete, F., Woldemichael, D.E., Gebremedhen, H.S., Batu, T. (2025). Free and Open-Source Python-Based Software Packages for Digital Image Correlation in Full-Field Displacement and Strain Measurements, Strain, 61(4), p. e70012. DOI: https://doi.org/10.1111/str.70012
[56] Kumar, S.S., Htike, M.H., Partanen, J., Almeida, J.H.S. (2025). Interfacial adhesion and failure transition governed by fibre embedded length in 3D-printed continuous carbon fibre–reinforced PETG composites, Journal of Thermoplastic Composite Materials.DOI: https://doi.org/10.1177/08927057251408473;WGROUP:STRING:PUBLICATION
[57] Kumar, V., Bharat, N., Mishra, V., Veeman, D., Vellaisamy, M. (2025). Flexural Strength Evolution of 3D-Printed PLA Structures: An Experimental Investigation, JOM, 77(4), pp. 2043–2053. DOI: https://doi.org/10.1007/s11837-024-07092-2
[58] Lei, J., Mei, S., Zhao, Q., Qiu, W. De., Wan, L. Bin., Wen, G.J. (2025). At-dicnet: a novel framework based speckle pattern for non-contact micron-level tool vibration deformation precision measurement, Journal of Intelligent Manufacturing, pp. 1–17. DOI: https://doi.org/10.1007/s10845-025-02723-0
[59] Li, R., Zhou, Y., Xu, Y., Zhou, L., Yang, B., Liu, Z., Liu, Y., Tang, L., Jiang, Z. (2025). Image feature guided self-adaptive subset configuration for digital image correlation, Opt. Laser Technol., 190, p. 113240. DOI: https://doi.org/10.1016/j.optlastec.2025.113240
[60] Liu, R., Xie, X., Wang, Q., Zhang, L., Yan, X. (2025). Fabrication of microscale heat-resistant and customizable speckles for deformation measurement using digital image correlation, Opt. Laser Technol., 192, p. 113814. DOI: https://doi.org/10.1016/j.optlastec.2025.113814
[61] Lu, H., Cary, P.D. (2000). Deformation measurements by digital image correlation: Implementation of a second-order displacement gradient, Experimental Mechanics 2000 40:4, 40(4), pp. 393–400. DOI: https://doi.org/10.1007/BF02326485
[62] Lu, L., Hou, J., Yuan, S., Yao, X., Li, Y., Zhu, J. (2023). Deep learning-assisted real-time defect detection and closed-loop adjustment for additive manufacturing of continuous fiber-reinforced polymer composites, Robot. Comput. Integr. Manuf., 79, p. 102431. DOI: https://doi.org/10.1016/j.rcim.2022.102431
[63] Luo, F., Kong, X., Jin, Z., Wang, P., Zhou, H., Zhu, Z., Gao, H. (2023). Investigation of the 3D-DIC testing method for composite shell in a deep-water high-pressure environment, Thin-Walled Structures, 190, p. 110962. DOI: https://doi.org/10.1016/j.tws.2023.110962

[64] Lupone, F., Padovano, E., Venezia, C., Badini, C. (2022). Experimental Characterization and Modeling of 3D Printed Continuous Carbon Fibers Composites with Different Fiber Orientation Produced by FFF Process, Polymers, 14(3). DOI: https://doi.org/10.3390/polym14030426
[65] Ma, L., Sun, H., Dong, X., Liu, Z., Wang, B. (2025). Bending-Induced Progressive Damage of 3D-Printed Sandwich-Structured Composites by Non-Destructive Testing, Polymers, 17(14). DOI: https://doi.org/10.3390/polym17141936
[66] Machado, V.J. da S., Cardoso, D.C.T. (2025). An Approach to FFF Elastic Properties Based on Classical Laminate Theory, Polym. Eng. Sci., 66(2), pp. 1309–1328. DOI: https://doi.org/10.1002/pen.70279
[67] Majid, F., Hachimi, T., Rhanim, H., Rhanim, R. (2023). Delamination effect on the mechanical behavior of 3D printed polymers, Frattura Ed Integrità Strutturale, 17(63), pp. 26–36. DOI: https://doi.org/10.3221/IGF-ESIS.63.03
[68] Maqsood, N., Rimašauskas, M. (2021). Delamination observation occurred during the flexural bending in additively manufactured PLA-short carbon fiber filament reinforced with continuous carbon fiber composite, Results in Engineering, 11, p. 100246. DOI: https://doi.org/10.1016/J.RINENG.2021.100246
[69] Mejia, E.B., McDougall, L., Gonsalves, N., Darby, D.R., Greenlee, A.J., Commisso, A., Johnson, J.A., Sottos, N., Appelhans, L.N., Cook, A.W., Leguizamon, S.C., Roach, D.J. (2025). Real-time process monitoring and automated control for direct ink write 3D printing of frontally polymerizing thermosets, Npj Advanced Manufacturing, 2(1), pp. 18. DOI: https://doi.org/10.1038/s44334-025-00032-1
[70] Minamino, T., Mine, A., Omiya, K., Matsumoto, M., Nakatani, H., Iwashita, T., Ohmi, M., Awazu, K., Yatani, H. (2014). Nondestructive observation of teeth post core space using optical coherence tomography: a pilot study, J. Biomed. Opt., 19(4), p. 046004. DOI: https://doi.org/10.1117/1.jbo.19.4.046004
[71] Mishra, V., Bharat, N., Veeman, D., Negi, S., Kumar, V. (2025). Statistical and machine-learning models to predict the flexural properties of wood-based composites fabricated via material extrusion technique, Wood Mater. Sci. Eng. DOI: https://doi.org/10.1080/17480272.2025.2488960
[72] Mishra, V., Negi, S., Bharat, N., Veeman, D., Kumar, V. (2026). Effect of FFF parameters on PLA/WD composite properties: Comparative analysis using Taguchi and GRA approach, Journal of Reinforced Plastics and Composites. DOI: https://doi.org/10.1177/07316844251314979
[73] Mishra, V., Negi, S., Kar, S. (2023). FDM-based additive manufacturing of recycled thermoplastics and associated composites, J. Mater. Cycles Waste Manag., 25(2), pp. 758–784.
[74] Naboulsi, N., Majid, F., Hachimi, T., Dadoun, S., Barhoumi, N., Khlifi, K. (2025). Predicting the strength of 3D-printed conductive composite under tensile load: A probabilistic modeling and experimental study, Fracture and Structural Integrity, 19(72), pp. 247–262. DOI: https://doi.org/10.3221/IGF-ESIS.72.18
[75] Németh, A., Ibrahim, S.K., Movahedi Rad, M., Szalai, S., Major, Z., Kocsis Szürke, S., Jóvér, V., Sysyn, M., Kurhan, D., Harrach, D., Baranyai, G., Fekete, I., Nagy, R., Csótár, H., Madarász, K., Pollák, A., Molnár, B., Hermán, B., Kuczmann, M., Gáspár, L., Fischer, S. (2024). Laboratory and Numerical Investigation of Pre-Tensioned Reinforced Concrete Railway Sleepers Combined with Plastic Fiber Reinforcement, Polymers (Basel)., 16(11). DOI: https://doi.org/10.3390/polym16111498
[76] Netto, J.V.B., Silva, É.H.P., Christoff, B.G., Ribeiro, M.L., Almeida, J.H.S. (2026). Fibre orientation-dependent damage modelling and experimental identification for 3D-printed continuous carbon fibre reinforced nylon composites, Mechanics of Materials, 218, p. 105697. DOI: https://doi.org/10.1016/J.MECHMAT.2026.105697
[77] Nguyen, T.D., Nguyen, M.T.N., Lee, J.S. (2025). Dynamic Covalent Bonds in 3D-Printed Polymers: Strategies, Principles, and Applications, Applied Sciences, 15(21). DOI: https://doi.org/10.3390/app152111755
[78] Pahari, S., Melenka, G.W. (2025). Analysis of the interface properties of multi-material fused filament fabricated (FFF) printed polymer composite structures, Int. J. Adhes. Adhes., 142, p. 104074. DOI: https://doi.org/10.1016/j.ijadhadh.2025.104074
[79] Pahlavani, H., Amani, M., Saldívar, M.C., Zhou, J., Mirzaali, M.J., Zadpoor, A.A. (2022). Deep learning for the rare-event rational design of 3D printed multi-material mechanical metamaterials, Communications Materials, 3(1), pp. 46-. DOI: https://doi.org/10.1038/s43246-022-00270-2
[80] Palanca, M., Tozzi, G., Cristofolini, L. (2016). The use of digital image correlation in the biomechanical area: A review, Int. Biomech., 3(1), pp. 1–21. DOI: https://doi.org/10.1080/23335432.2015.1117395
[81] Pan, B. (2018). Digital image correlation for surface deformation measurement: historical developments, recent advances and future goals, Meas. Sci. Technol., 29(8), p. 082001. DOI: https://doi.org/10.1088/1361-6501/aac55b
[82] Pan, B. (2014). An evaluation of convergence criteria for digital image correlation using inverse compositional Gauss-Newton algorithm, Strain, 50(1), pp. 48–56. DOI: https://doi.org/10.1111/str.12066
[83] Pan, B. (2009). Reliability-guided digital image correlation for image deformation measurement, Applied Optics, 48(8), pp. 1535–1542. DOI: https://doi.org/10.1364/AO.48.001535

[84] Pellegrini, A., Palmieri, M.E., Guerra, M.G. (2022). Evaluation of anisotropic mechanical behaviour of 316L parts realized by metal fused filament fabrication using digital image correlation, The International Journal of Advanced Manufacturing Technology, 120(11), pp. 7951–7965. DOI: https://doi.org/10.1007/s00170-022-09303-z
[85] Perez, D.B., Celik, E., Karkkainen, R.L. (2021). Investigation of Interlayer Interface Strength and Print Morphology Effects in Fused Deposition Modeling 3D-Printed PLA, 3D Print. Addit. Manuf., 8(1), pp. 23–32. DOI: https://doi.org/10.1089/3dp.2020.0109
[86] Peters, W.H., Ranson, W.F. (1982). Digital Imaging Techniques In Experimental Stress Analysis, Optical Engineering, 21(3). DOI: https://doi.org/10.1117/12.7972925
[87] Piepoli, A., Lagrasta, F.P., Pellegrino, R., Pontrandolfo, P. (2025). Recycled vs. Virgin Materials in Additive Manufacturing: Assessing the Risk Mitigation Potential in Uncertain Supply Scenarios, Procedia Comput. Sci., 253(2), pp. 2605–2614. DOI: https://doi.org/10.1016/j.procs.2025.01.320
[88] Popławski, A., Bogusz, P., Grudnik, M. (2025). Digital Image Correlation and Numerical Analysis of Mechanical Behavior in Photopolymer Resin Lattice Structures, Materials, 18(2). DOI: https://doi.org/10.3390/ma18020384
[89] Pureza, D.Q., de Brito, J.L.V., Alencar, G.S., Veloso, L.A.C.M. (2026). DICLab2D: An open-source digital image correlation algorithm for Julia language, SoftwareX, 33(6), p. 102532. DOI: https://doi.org/10.1016/j.softx.2026.102532
[90] Rahman, M.S., Alam, C.S., Pulok, M.K.H., Zeng, C., Chakravarty, U.K. (2025). An Investigation of Tensile, Fatigue, and Fracture Behavior of 3D-Printed Polymers, J. Eng. Mater. Technol., 147(1). DOI: https://doi.org/10.1115/1.4065958
[91] Reu, P.L., Blaysat, B., Andó, E., Bhattacharya, K., Couture, C., Couty, V., Deb, D., Fayad, S.S., Iadicola, M.A., Jaminion, S., Klein, M., Landauer, A.K., Lava, P., Liu, M., Luan, L.K., Olufsen, S.N., Réthoré, J., Roubin, E., Seidl, D.T., Siebert, T., Stamati, O., Toussaint, E., Turner, D., Vemulapati, C.S.R., Weikert, T., Witz, J.F., Witzel, O., Yang, J. (2022). DIC Challenge 2.0: Developing Images and Guidelines for Evaluating Accuracy and Resolution of 2D Analyses: Focus on the Metrological Efficiency Indicator, Exp. Mech., 62(4), pp. 639–654. DOI: https://doi.org/10.1007/s11340-021-00806-6
[92] Rezaie, A., Achanta, R., Godio, M., Beyer, K. (2020). Comparison of crack segmentation using digital image correlation measurements and deep learning, Constr. Build. Mater., 261, p. 120474. DOI: https://doi.org/10.1016/J.CONBUILDMAT.2020.120474
[93] Sadeghian, M., Palevicius, A., Sablinskas, J., Griskevicius, P. (2025). From Pixels to Predictions: Integrating Machine Learning and Digital Image Correlation for Damage Identification in Engineering Materials, Materials, 19(1). DOI: https://doi.org/10.3390/ma19010077
[94] Schreier, H.W., Braasch, J.R., Sutton, M.A. (2000). Systematic errors in digital image correlation caused by intensity interpolation, 39(11), pp. 2915–2921. DOI: https://doi.org/10.1117/1.1314593
[95] Schreier, H.W., Sutton, M.A. (2002). Systematic errors in digital image correlation due to undermatched subset shape functions, Experimental Mechanics, 42(3), pp. 303–310. DOI: https://doi.org/10.1007/BF02410987
[96] Seifollahi, M., Kabir, M.Z. (2025). Fatigue Life Assessment of Notched PLA Manufactured Using FDM 3D-Printing Technique, Polymers, 18(1). DOI: https://doi.org/10.3390/polym18010001
[97] Shahan, H.T., Zainuddin, S., Harry, R., Baig, Z., Sayeed, G.M. (2025). Evaluating Mechanical Integrity of 3D-Printed PLA and ABS by Varying Process Parameters, Journal of Materials Engineering and Performance, 35(3), pp. 2439–2448. DOI: https://doi.org/10.1007/s11665-025-11785-3
[98] Su, Y., Lao, L. (2024). Modeling the measurement accuracy of one-dimensional boundary subsets in digital image correlation, Opt. Lasers Eng., 181, p. 108362. DOI: https://doi.org/10.1016/j.optlaseng.2024.108362
[99] Sutton, M., Wolters, W., Peters, W., Ranson, W., McNeill, S. (1983). Determination of displacements using an improved digital correlation method, Image Vis. Comput., 1(3), pp. 133–139. DOI: https://doi.org/10.1016/0262-8856(83)90064-1
[100] Szalai, S., Szívós, B.F., Kurhan, D., Németh, A., Sysyn, M., Fischer, S. (2023). Optimization of Surface Preparation and Painting Processes for Railway and Automotive Steel Sheets, Infrastructures, 8(2). DOI: https://doi.org/10.3390/infrastructures8020028
[101] Tang, C., Liu, J., Hao, W., Wei, Y. (2023). Flexural properties of 3D printed graded lattice reinforced cementitious composites using digital image correlation, Mater. Des., 227(16), p. 111734. DOI: https://doi.org/10.1016/j.matdes.2023.111734
[102] Taoufik, H., Hmazi, F.A., Arhouni, F.E., Rejdali, H., Riyad, Y., Majid, F. (2026). Experimental calibration of a virtual raster section for high-accuracy FDM simulation in Abaqus, Fracture and Structural Integrity, 20(76), pp. 31–48. DOI: https://doi.org/10.3221/IGF-ESIS.76.03

[103] Timpano, C.S., Melenka, G.W. (2021). Digital volume correlation analysis of polylactic acid based fused filament fabrication printed composites, J. Compos. Mater., 55(25), pp. 3699–3717. DOI: https://doi.org/10.1177/00219983211020500
[104] Tong, W. (2005). An Evaluation of Digital Image Correlation Criteria for Strain Mapping Applications, Strain, 41(4), pp. 167–175. DOI: https://doi.org/10.1111/J.1475-1305.2005.00227.X
[105] Turner, D., Crozier, P., Reu, P. (2015). Digital Image Correlation Engine v.3.0. DOI: https://doi.org/10.11578/DC.20171025.1658
[106] Venter, G., Neaves, M. (2025). SUN-DIC: A Python-based open-source software tool for Digital Image Correlation, Advances in Engineering Software, 211(1), p. 104043. DOI: https://doi.org/10.1016/j.advengsoft.2025.104043
[107] Wang, G., Zhou, Y., Wang, Z., Zhou, J., Xuan, S., Yao, X. (2024). StrainNet-LD: Large Displacement digital image correlation based on deep learning and displacement-field decomposition, Opt. Lasers Eng., 183, p. 108502. DOI: https://doi.org/10.1016/j.optlaseng.2024.108502
[108] Wang, L., Lei, Z. (2025). Deep learning based speckle image super-resolution for digital image correlation measurement, Opt. Laser Technol., 181, p. 111746. DOI: https://doi.org/10.1016/j.optlastec.2024.111746
[109] Wang, Y., Luo, Q., Xie, H., Li, Q., Sun, G. (2022). Digital image correlation (DIC) based damage detection for CFRP laminates by using machine learning based image semantic segmentation, Int. J. Mech. Sci., 230, p. 107529. DOI: https://doi.org/10.1016/J.IJMECSCI.2022.107529
[110] Wikło, M., Byczuk, B.H., Skrzek, K. (2025). Mechanical Characterization of FDM 3D-Printed Components Using Advanced Measurement and Modeling Techniques, Materials 18(5). DOI: https://doi.org/10.3390/ma18051086
[111] Xu, G., Yue, Q., Liu, X. (2023). Real-time monitoring of concrete crack based on deep learning algorithms and image processing techniques, Advanced Engineering Informatics, 58, p. 102214. DOI: https://doi.org/10.1016/j.aei.2023.102214
[112] Yang, R., Li, Y., Zeng, D., Guo, P. (2022). Deep DIC: Deep learning-based digital image correlation for end-to-end displacement and strain measurement, J. Mater. Process. Technol., 302, p. 117474. DOI: https://doi.org/10.1016/j.jmatprotec.2021.117474
[113] Yuan, Z., Lu, Y., Deng, K., Wang, Z., Wang, X. (2025). Multi-level feature fusion DIC model for in-situ measurement of kinematic fields during milling process, J. Manuf. Process., 152, pp. 1310–1328. DOI: https://doi.org/10.1016/j.jmapro.2025.08.075
[114] Zappino, E., Filippi, M., Pagani, A., Petiti, M., Carrera, E. (2020). Experimental and numerical analysis of 3D printed open-hole plates reinforced with carbon fibers, Composites Part C: Open Access, 2, p. 100007. DOI: https://doi.org/10.1016/j.jcomc.2020.100007
[115] Zappino, E., Zobeiry, N., Petrolo, M., Vaziri, R., Carrera, E., Poursartip, A. (2020). Analysis of process-induced deformations and residual stresses in curved composite parts considering transverse shear stress and thickness stretching, Compos. Struct., 241, p. 112057. DOI: https://doi.org/10.1016/j.compstruct.2020.112057
[116] Zekriti, N., Majid, F., Taoufik, H., Tounsi, Y., Rhanim, R., Mrani, I., Rhanim, H. (2023). Improvement of crack tip position estimation in DIC images by image processing methods, Frattura Ed Integrità Strutturale, 17(63), pp. 61–71. DOI: https://doi.org/10.3221/IGF-ESIS.63.06
[117] Zhou, T., Chen, J., Xie, H., Zhou, C., Wang, F., Zhu, J. (2022). Failure and Mechanical Behaviors of Sandstone Containing a Pre-existing Flaw Under Compressive–shear Loads: Insight from a Digital Image Correlation (DIC) Analysis, Rock Mechanics and Rock Engineering 2022 55:7, 55(7), pp. 4237–4256. DOI: https://doi.org/10.1007/s00603-022-02861-4
[118] Zhou, Y., Zhang, X., Zhao, Z. (2025). DICNO: A Generalizable Digital Image Correlation Neural Operator, IEEE Trans. Instrum. Meas., 74. DOI: https://doi.org/10.1109/TIM.2025.3612640
[119] Zhou, Y., Zuo, Q., Chen, N., Zhou, L., Yang, B., Liu, Z., Liu, Y., Tang, L., Dong, S., Jiang, Z. (2025). Transformer based deep learning for digital image correlation, Opt. Lasers Eng., 184, p. 108568. DOI: https://doi.org/10.1016/j.optlaseng.2024.108568
[120] Zouaoui, M., Gardan, J., Lafon, P., Makke, A., Labergere, C., Recho, N. (2021). A Finite Element Method to Predict the Mechanical Behavior of a Pre-Structured Material Manufactured by Fused Filament Fabrication in 3D Printing, Applied Sciences 11(11), p. 5075. DOI: https://doi.org/10.3390/APP11115075